

1 Does drought advance the onset of
2 autumn leaf senescence in temperate
3 deciduous forest trees?
4
5

6 Bertold Mariën^{1,*}, Inge Dox¹, Hans J De Boeck¹, Patrick Willems², Sebastien Leys¹, Dimitri Papadimitriou³ and Matteo
7 Campioli¹

8 ¹PLECO (Plants and Ecosystems), Department of Biology, University of Antwerp, 2160 Wilrijk, Belgium

9 ²Hydraulics Division, KU Leuven, Kasteelpark Arenberg 40, 3001, Leuven, Belgium

10 ³IDLab (Internet Data Lab), Department of Mathematics and Computer Science, University of Antwerp, 2000 Antwerp, Belgium
11
12

13

14 *Author for correspondence:

15 *Bertold Mariën*

16 *Tel: 032659333*

17 *Email: bertold.marien@uantwerpen.be*
18

19

20 Abstract

- 21 • Severe droughts are expected to become more frequent and persistent. However, their effect on
22 autumn leaf senescence, a key process for deciduous trees and ecosystem functioning, is currently
23 unclear. We hypothesized that (I) severe drought advances the onset of autumn leaf senescence
24 in temperate deciduous trees and that (II) tree species show different dynamics of autumn leaf
25 senescence under drought.
- 26 • We tested these hypotheses using a manipulative experiment on beech saplings and three years
27 of monitoring mature beech, birch and oak trees in Belgium. The autumn leaf senescence was
28 derived from the seasonal pattern of the chlorophyll content index and the loss of canopy
29 greenness using generalized additive models and piece-wise linear regressions.
- 30 • Drought and associated heat stress and increased atmospheric aridity did not affect the onset of
31 autumn leaf senescence in both saplings and mature trees, even if the saplings showed a high
32 mortality and the mature trees an advanced loss of canopy greenness. We did not observe major
33 differences among species.
- 34 • Synthesis: The timing of autumn leaf senescence appears conservative across years and species,
35 and even independent of drought, heat and increased atmospheric aridity. Therefore, to study
36 autumn senescence and avoid confusion among studies, seasonal chlorophyll dynamics and loss
37 of canopy greenness should be considered separately.

63 Key words

64 Autumn leaf senescence, *Betula pendula*, Drought, Heat stress and increased atmospheric aridity , *Fagus*
65 *sylvatica*, Generalized additive mixed models, Leaf coloration and fall, *Quercus robur*, Rainfall deficit

66 1. Introduction

67 Autumn leaf senescence is a developmental stage of the leaf cells. The core function of this process is the
68 remobilization of nutrients and death is its consequence (Medawar, 1957;Keskitalo et al., 2005). Its
69 evolutionary purpose is likely stress resistance and, as such, the process dynamics are affected by different
70 forms of environmental stress (e.g. high temperatures, water logging) (Benbella and Paulsen, 1998;Leul
71 and Zhou, 1998;Munné-Bosch and Alegre, 2004). The process of autumn leaf senescence is highly
72 coordinated and characterized by a tight control over its timing. Furthermore, its most manifest feature,
73 the detoxification of chlorophyll, allows the degradation of leaf macromolecules and subsequent nutrient
74 remobilization -the essence of autumn leaf senescence- (Hörtensteiner and Feller, 2002;Munné-Bosch
75 and Alegre, 2004;Matile, 2000). In addition, chlorophyll degradation allows for the typical leaf coloration
76 during autumn. However, autumn leaf senescence is also an important process at the ecosystem scale
77 because it affects multiple ecological processes, such as trophic dynamics, tree growth or the exchange
78 of matter and energy between the ecosystem and atmosphere (Richardson et al., 2013).

79
80 Literature reports several definitions of autumn senescence and of multiple observational methods to
81 measure autumn senescence (Gill et al., 2015;Fracheboud et al., 2009;Gallinat et al., 2015). This has
82 hampered our understanding of the effects of drought stress on the timing of the onset of autumn leaf
83 senescence, as opposed to the timing of leaf abscission or accelerated leaf senescence. For example,
84 Estiarte and Penuelas (2015) reported that leaf senescence advances due to drought stress, while Vander
85 Mijnsbrugge et al. (2016) reported a delay in the leaf senescence of young trees subjected to drought.
86 After the summer drought in central Europe of 2003, Leuzinger et al. (2005) even reported that the leaf
87 longevity (measured as a delay in the leaf discoloration and fall) of five deciduous tree species was on
88 average prolonged by 22 days.

89
90 Droughts are expected to occur more frequently and become more intensive due to global warming and
91 changes in precipitation patterns (IPCC, 2014;Crabbe et al., 2016). Extended periods with lower than
92 average rainfall are often associated with higher air temperatures and higher vapor pressure deficits,
93 which can negatively affect the functioning of trees in the temperate zone (Novick et al., 2016;De Boeck
94 and Verbeeck, 2011). Belgian forests are thought to be especially vulnerable to droughts as they typically
95 have sandy soils with low soil field capacities (Vander Mijnsbrugge et al., 2016;van der Werf et al., 2007).

96
97 To examine the effects of drought stress on the onset of autumn leaf senescence, we hypothesized that:

- 98 (I) the timing of the onset of autumn leaf senescence in temperate deciduous trees is advanced
99 by severe drought stress. The leaves of a tree that experiences drought will accumulate the
100 consequences of stress exposure and lose functionality. Therefore, it is likely not beneficial
101 for a tree to maintain active leaves late in the season after severe drought. Instead, to
102 maximize nutrient recovery, trees probably prefer an earlier leaf senescence. In addition,
103 drought would reduce the tree's wood growth and increase its fine root mortality (Brunner
104 et al., 2015;Capioli et al., 2013). Consequently, the tree's carbon sink strength will decline,
105 causing a reduced demand for carbon from the sources (e.g. the leaves) and advance the
106 onset of autumn leaf senescence.
- 107 (II) different tree species show different dynamics in their onset of autumn leaf senescence under
108 drought. We hypothesized that, under drought stress, species with continuous flushing (e.g.
109 birch) will have a more stable timing onset of autumn leaf senescence than species with only
110 one or two leaf flushes during spring-summer (e.g. beech and oak) (Koike, 1990).

111

112 We tested these hypotheses by subjecting young trees to treatments comprising less irrigation and
113 warming, and by examining the effect of years with different drought intensities (2017, 2018 and 2019)
114 on mature trees in natural forest stands. Both young and mature trees experienced not only drought, but
115 also heat and increased atmospheric aridity.

116 2. Materials and methods

117 2.1. Study sites and experimental setting

118 2.1.1. Manipulative experiment

119 In 2018, we carried out a manipulative experiment at the Drie Eiken Campus in Wilrijk, Belgium (51°09'N,
120 4°24'E). In early March, 128 individuals of three-year-old beech (*Fagus sylvatica*) saplings, from a local
121 nursery and with the same local provenance, were planted in pots with a volume of 35 liters and a surface
122 area of 0.07 m². The pots were filled with 20% peat and 80% white sand. Eight beech saplings were placed
123 in each of twelve climate-controlled glasshouses with a ground surface of 1.5 x 1.5 m and a height at the
124 north and south side of 1.5 m and 1.2 m, respectively. The glasshouses had a roof of colorless
125 polycarbonate (a 4 mm thick plate) reducing the incoming light by ± 20% and modifying the spectral
126 quality only in the UV range (Kwon et al., 2017). The glasshouses had three sides that could be opened or
127 closed and were equipped with a combined humidity-temperature sensor (QFA66, Siemens, Erlangen,
128 Germany) to monitor the relative humidity and air temperature (Fig. 1, panel A and B) (Kwon et al., 2017).
129 One pot per glasshouse was also equipped with a soil moisture smart sensor (HOBO S-SMD-M005, Onset,
130 MA, USA) to monitor the soil water content (Fig. 1, panel C). The latter sensors became available only at
131 the time the drought stress was alleviated (see below). More details on the set-up of the glasshouses can
132 be found in the literature (Van den Berge et al., 2011; De Boeck et al., 2012; Fu et al., 2014). Two treatments
133 were organized (n = 48 per treatment; see below). In addition to the saplings in the glasshouses, eight
134 beech saplings were placed in each of four reference plots outside of the glasshouses (n = 32, Ref.). The
135 relative humidity and air temperature of the outside reference plots were monitored by a pocket weather
136 meter (Kestrel 3000, Nielsen, PA, USA). Once in April and once in July, all saplings received 35 g of NPK
137 slow-release fertilizer (DCM ECO-XTRA 1) and 1.8 g of micro elements (DCM MICRO-MIX). Using the
138 relative humidity and air temperature data between 7 a.m. and 7 p.m., the vapor pressure deficit was
139 calculated for both treatments (see below) and the reference plots using the formulas of Buck (1981) (Eq.
140 1; Fig. 1, panel D).

141

142 Equation 1

$$143 e_0 = 613.75 \times \exp((17.502 \times T)/(240.97 + T))$$

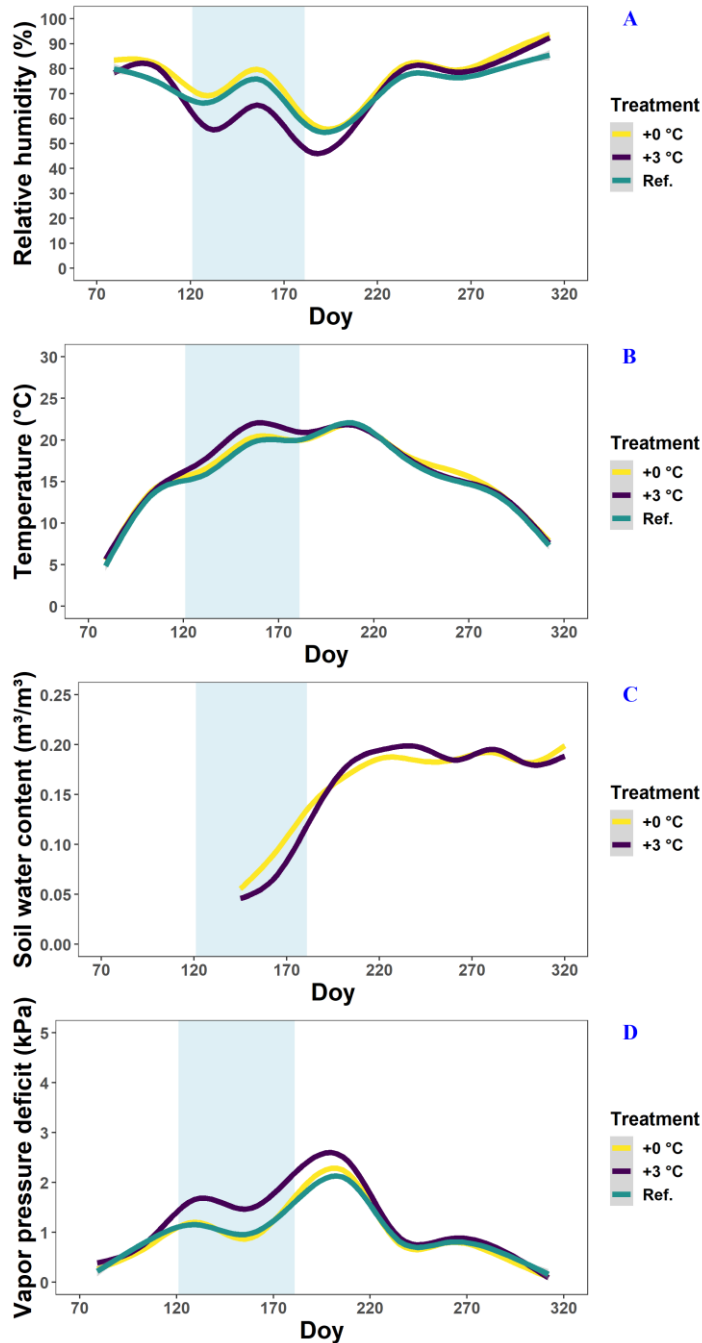
$$144 e = (RH/100) \times e_0$$

$$145 VPD = e_0 - e$$

146

147 where e_0 is the saturation vapor pressure (in Pa), T is the temperature (in °C), e is the actual vapor pressure
148 deficit (in Pa), RH is the relative humidity (in %) and VPD is the vapor pressure deficit (in Pa).

149



150
 151 Fig. 1: The relative humidity (panel A), temperature (panel B), soil water content (panel C) and vapor
 152 pressure deficit (panel D) in the glasshouses and outside plots at the Drie Eiken Campus in Wilrijk. Solid
 153 lines represent regressions of half-hourly measurements of the relative humidity (%), temperature (°C),
 154 and soil water content (m³/m³). Regressions were done using generalized additive models implemented
 155 by the *geom_smooth* argument in the R/GGPlot2 package. The vapor pressure deficit (kPa) was calculated
 156 using the formulas of Buck (1981) using data of the relative humidity and air temperature between 7 a.m.
 157 and 7 p.m. Green, blue and red lines represent the conditions in the reference plots (Ref.), glasshouses
 158 that follow the outside ambient air temperature (+0 °C) and glasshouses that are three degrees warmer
 159 than the outside ambient air temperature (+3 °C), respectively. The light blue band represents the
 160 treatment-period.

161 From planting until April, the saplings were all irrigated two to three times a week until the pots
162 overflowed. The reference plots outside were maintained with abundant irrigation during the whole
163 growing season. On the other hand, at the start of the treatment, in early May, we shielded all the
164 glasshouses using polyethylene film (200 μm thick) and irrigated the saplings only once a week with circa
165 2.5 liter of water. In addition, we enhanced the drought in six glasshouses by raising the air temperature
166 three degrees compared to the ambient air temperature (+3 $^{\circ}\text{C}$). The air temperature in the other six
167 glasshouses followed the ambient air temperature (+0 $^{\circ}\text{C}$). There were no significant differences in the
168 temperature, relative humidity and vapor pressure deficit among the glasshouses with the reference and
169 +0 $^{\circ}\text{C}$ treatment (Fig. 1). Although no data on the soil water content was available for the reference plots
170 (due to sensor malfunctioning), we did not expect major drought stress due to their abundant irrigation
171 and lack of stress signals. Based on this information, the +0 $^{\circ}\text{C}$ treatment can be considered a ‘less-
172 irrigation/drought’ treatment. On the other hand, during the treatment, the daily soil water content and
173 the daily relative humidity in the glasshouses with the +3 $^{\circ}\text{C}$ treatment were significantly lower ($P < 0.001$;
174 tested using generalized additive mixed models) in comparison to the glasshouses with the +0 $^{\circ}\text{C}$
175 treatment. After statistical testing following Rose et al. (2012), the difference between the +0 $^{\circ}\text{C}$ and +3
176 $^{\circ}\text{C}$ treatments was found to be around 0.025 m^3/m^3 for the soil water content and 20% for the relative
177 humidity (Fig. 1; see Data availability). The +3 $^{\circ}\text{C}$ treatment can therefore be considered a combined ‘less-
178 irrigation/drought, warming and increased atmospheric aridity’ treatment. In fact, this treatment should
179 simulate natural drought conditions, which are often associated with heat stress and increased
180 atmospheric aridity. The plan was to continue the treatment till the end of June but, due to the significant
181 mortality rate, we were obliged to alleviate the drought already from the 20th of June by increasing the
182 irrigation to the level of the reference plots. From July, the glasshouses were opened again and the
183 saplings were irrigated four to five times a week until the end of the season.

184
185 A draw-back of the experiment is that the saplings in the reference plots received more incoming light
186 (i.e. $\pm 20\%$) than the saplings in the glasshouses (Van den Berge et al., 2011). However, as beech is a shade
187 tolerant species, reduced light is unlikely to have limited tree growth. In addition, preliminary tests
188 suggested that the ratio of light in different wavelengths (e.g. R/FR) during civil twilight (i.e. what is
189 required for phytochrome to detect the photoperiod) does not change seasonally significantly in our study
190 area (Chelle et al., 2007).

191

192 2.1.2. Field observations in deciduous forests

193 From 2017 to 2019, we monitored dominant mature trees in two forests near Antwerp: the Klein
194 Schietveld in Kapellen (KS; 51°21'N, 4°37'E) and the Park of Brasschaat (PB; 51°12'N", 4°26'E). In the KS,
195 we monitored eight beech trees and eight birch (*Betula pendula*) trees. In the PB, we monitored eight
196 beech trees and eight oak (*Quercus robur*) trees (thus 32 trees in total). The two forests and their
197 meteorological conditions are described in detail by Mariën et al. (2019), which also showed a lack of site
198 effects on the autumn chlorophyll dynamics for the tree species studied here. To have a larger statistical
199 sample, the data of the two beech stands (also of similar age and stem diameter) were aggregated.

200

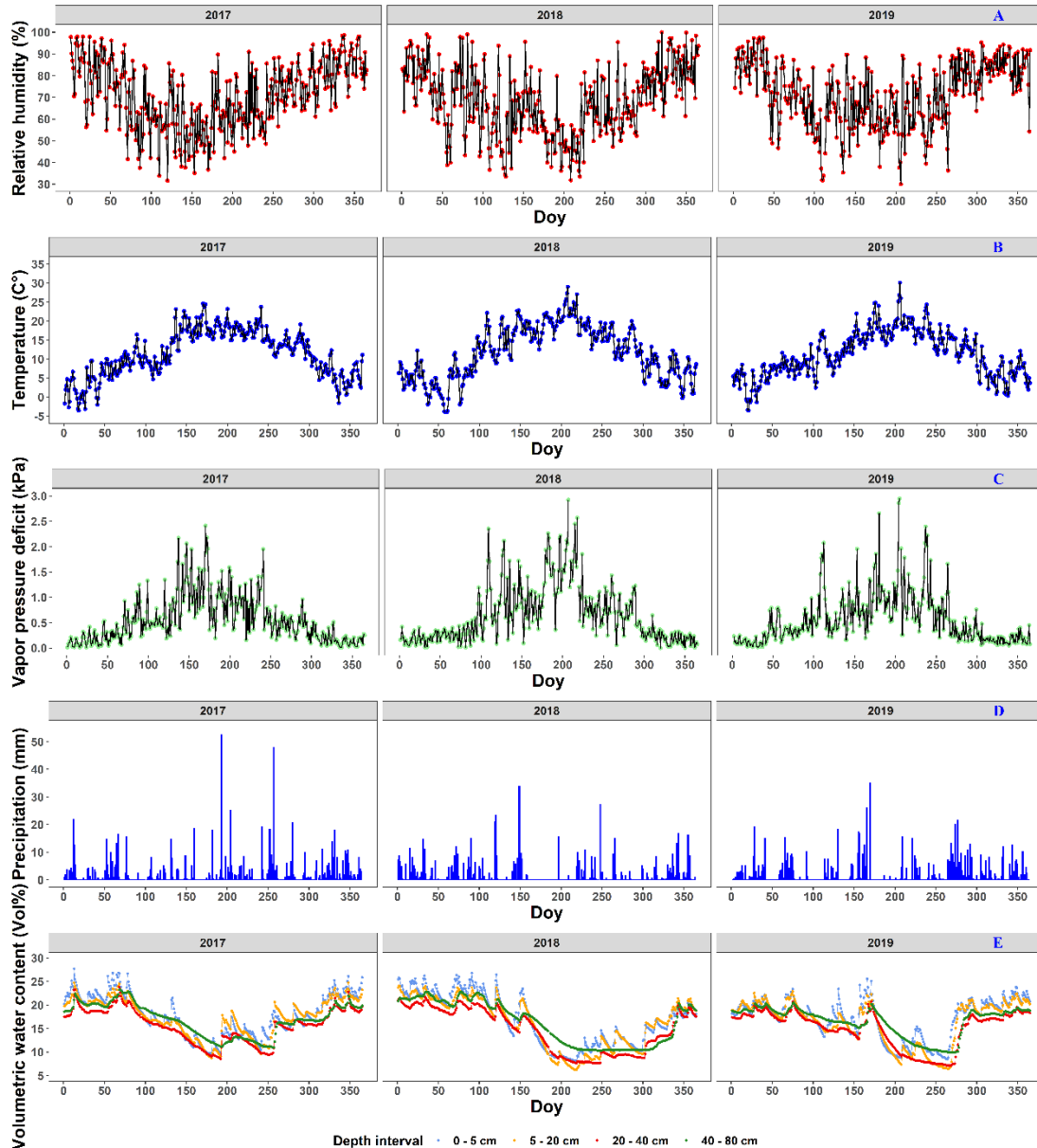
201 For summer and autumn, we report here the average values for the temperature, precipitation, number
202 of rainy days, relative humidity, sunshine duration and global solar radiation for the meteorological station
203 of the Royal Meteorological Institute (KMI) in Ukkel, Belgium (Table 1). For these data, long-term averaged
204 data was available. The temperature, relative humidity, vapor pressure deficit (see Eq. 1), precipitation
205 and volumetric soil water content from 2017 to 2019 are presented in more detail using daily values that
206 were measured at Brasschaat and, whenever necessary, gap-filled with data from the meteorological
207 station in Woensdrecht, Netherlands (Fig. 2, panel A – B; panel D). The meteorological data from
208 Brasschaat was provided by the Flemish Institute for Nature and Forest (INBO) and the Integrated Carbon

209 Observation System (ICOS), while the data from Woensdrecht was provided by the Royal Dutch
210 Meteorological Institute (KNMI).

211 Table 1: Overview of the meteorological conditions during the summer and autumn of 2017, 2018 and
 212 2019. All data is measured by the meteorological station of the Royal Meteorological Institute (KMI) in
 213 Ukkel, Belgium (KMI, 2018a, b, 2017b, c, 2019a, b). The degree of abnormality of the values is represented
 214 by two labels: a for abnormal values (with a recurrence time of six years) or e for exceptional values (with
 215 a recurrence time of thirty years). In case only one month had abnormal values, this label is followed by
 216 the name of that particular month. Since 2019, the KMI uses a new system to show the degree of
 217 abnormality: values that are with the five highest values since 1981 are marked by (+), while values within
 218 the three highest values are marked by (++)
 219

	Normal (1981-2010)		2017		2018		2019	
	summer	autumn	summer	autumn	summer	autumn	summer	autumn
Average temperature (°C)	17.6	10.9	18.6 (a)	11.3	19.8 (e)	11.8	19.1 (++)	11.3
Total precipitation (mm)	224.6	219.9	179.9	226.5	134.7 (a)	168.5	198.6	209.3
Average number of rainy days	43.9	51	44	63 (a)	20 (e)	32 (e)	33	53
Relative humidity (%)	73	82	67.7 (e, June)	62	62.3 (e, July)	75 (e, July)	70	83
Sunshine duration (h:m)	578:20	322:00	573:21	322:00	693:06 (a)	471:12 (e)	714:38 (++)	322:23
Global solar radiation (kWh/m²)	429.6	168.2	447.1 (a, June)	233.8	498.6 (e, July)	213.4 (e, October)	487.9 (+)	178.4

220



221

222 Fig. 2: The meteorological conditions near the Klein Schietveld and Park of Brasschaat. The line plots
 223 represent the daily average relative humidity (%; red), temperature (°C; blue) and vapor pressure deficit
 224 (kPa; green). The bar plots represent the daily precipitation (mm; light blue). The volumetric soil water
 225 content (Vol%) at depth intervals of 0 – 5 cm, 5 – 20 cm, 20 – 40 cm and 40 – 80 cm is presented as line
 226 plots in cornflower blue, orange, red and green, respectively. The relative humidity, temperature, vapor
 227 pressure deficit and precipitation data was measured every half hour and provided by the Flemish
 228 Institute for Nature and Forest (INBO), the Integrated Carbon Observation System (ICOS) and the Royal
 229 Dutch Meteorological Institute (KNMI). The vapor pressure deficit (kPa) was calculated using the formulas
 230 of Buck (1981) using data of the relative humidity and air temperature between 7 a.m. and 7 p.m. The
 231 volumetric soil water content data was first measured every six hours but after 03/07/2018
 232 measurements were made every hour. The volumetric soil water content data was provided through
 233 courtesy of INBO.

234

235 The distance from Ukkel and Woensdrecht to our sites is 60 km and 20 km, respectively. However, both
236 locations show no major climatological differences with the KS and PB, and are representative for the
237 inter-annual variability experienced by the forests. The station of Ukkel is located within a green area in
238 the suburb of Brussels (thus, classifiable as “urban park”). The microclimate is expected to be different
239 than at our study sites. However, data from Ukkel were used to describe the intra-annual variability and
240 long-term trends in the meteorological variables, which are less affected by the microclimate. The
241 meteorological station of Brasschaat is very close to our sampling site in the Park of Brasschaat and in the
242 Klein Schietveld (± 3 km and ± 4 km, respectively). The meteorological station in Brasschaat is a 40 m high
243 scaffolding tower, at which measurements are taken at various heights, and stands in a patch of mixed
244 forest covered mainly by Scots pines and deciduous tree species, such as oak and birch (see Carrara et al.
245 (2003) for more information). Data of the temperature, precipitation and humidity were taken at the top
246 of the tower. Concurrently, the volumetric soil water content was measured near the scaffolding tower
247 using twelve water reflectometers (CS616 Water Content Reflectometer, Campbell Scientific, UT, USA)
248 connected to a central data logger (CR1000 data logger, Campbell Scientific, UT, USA). The water
249 reflectometers were equally divided over three sampling pits at an 8 m distance from the central data
250 logger. In 2010 and in each pit, the water reflectometers were installed in pedogenetic horizons at four
251 depth intervals (i.e. 0 – 5 cm, 5 – 20 cm, 20 – 40 cm and 40 – 80 cm). The volumetric soil water content
252 data was first measured every six hours but after 03/07/2018 measurements were made every hour. The
253 volumetric soil water content was calibrated following De Vos (2016) and averaged per day and depth
254 interval. The station of Woensdrecht is located in an open field at a local airport surrounded by heathland
255 and urban area. It is located near the Markiezaatsmeer, an enclosed swamp ecosystem, within the river
256 mouth of the Schelde. The measurements in both Ukkel and Woensdrecht are taken at a height of 1.5 m.
257 However, these data were only used as gap-filling in case of short term gaps in the long-term Brasschaat
258 series.
259

260 *2.1.3. The rainfall deficit: an indicator of drought stress for 2017 - 2019*

261 To indicate the magnitude of the droughts, we computed the rainfall deficit from 2017 to 2019 using data
262 on the relative humidity, solar radiation, wind speed, temperature and precipitation from the
263 meteorological station in Ukkel. Here, the meteorological records go back the longest in Belgium. The
264 rainfall deficit is computed on a daily basis by accumulating the daily potential evapotranspiration minus
265 the daily amount of precipitation. This was done in two ways: (I) per hydrological year, starting from a
266 zero deficit at the start of the hydrological year (1st of April) and (II) continuous computation, so no restart
267 from 0 at the start of each hydrological year. The latter method has the benefit that the long-term effect
268 of accumulated droughts from successive years is accounted for.
269

270 The potential evapotranspiration was computed by means of the method of Bultot et al. (1983), which is
271 similar to the method of Penman (1948), but has parameters that are calibrated specifically for the local
272 Belgian conditions. Unlike for the rainfall deficit starting from a zero deficit, we accounted in the
273 calculation of the continuously computed rainfall deficit for the hydrological fraction in wet periods that
274 does not contribute to building up ground water reserves. At the station of Ukkel, daily precipitation and
275 potential evapotranspiration data are available since more than 100 years. The precipitation data are
276 collected since 1898 on the same location, and is measured using the same instrument. For this study, the
277 data for the 100-year period 1901-2000 was considered as the reference period for the computation of
278 long-term statistics on the rainfall deficit.
279

280 2.2. Measuring autumn leaf senescence: the chlorophyll content index and the loss of 281 canopy greenness

282 In the manipulative experiment from late-July until late-November, we measured the chlorophyll content
283 index (CCI; a proxy for the chlorophyll concentration) of each tree sapling weekly by randomly selecting
284 one leaf from the outer, middle and inner layer of the upper part of the crown. The CCI was measured
285 using a chlorophyll content meter, which measures the optical absorbance in the 653 nm and 931 nm
286 wavebands (CCM-200 plus, Opti-Sciences Inc., Hudson, NH, USA). Concurrently, we visually estimated the
287 loss of canopy greenness (LOCG; scaled between 0 and 1) of each sapling following the method of Vitasse
288 et al. (2011), which accounts for both the percentage of leaves that have changed color and the
289 percentage of leaves that have fallen.

290
291 For half of the monitored mature trees in the two forests and from the end of July to the end of November,
292 tree-climbers collected leaves on eight occasions per year separated by two to three weeks. During each
293 measurement day, they collected five sun-leaves and five shade-leaves from each tree. Afterwards, the
294 CCI was immediately measured on the harvested leaves using the same chlorophyll content meter as
295 described above. From early September to late November, the loss of canopy greenness was estimated
296 in a similar fashion to the manipulative experiment for the 32 mature trees (Vitasse et al., 2011).

297
298 Following the method of Mariën et al. (2019), we validated the CCI values by measuring also the
299 chlorophyll concentrations (Fig. A1). In 2017 and 2018, on one occasion per month and using a 10-mm
300 diameter cylinder, we collected samples of leaf tissue from the leaves of the mature trees for which we
301 also measured the CCI. After storage at -80 °C, the samples were grounded using glass beads and a
302 centrifuge. The result was dissolved in ethanol and the absorption of the solution was measured using a
303 spectrophotometer (Smart Spec Plus Spectrophotometer, Bio-Rad) at different wavelengths for
304 Chlorophyll a (662 nm) and chlorophyll b (644 nm). The chlorophyll concentrations could then be derived
305 from the absorption values using the formulas described in Holm (1954) and Vonwettstein (1957).

307 2.3. Tree mortality in the manipulative experiment

308 In this study, we only considered those trees that defoliated due to autumn leaf senescence. Other tree
309 saplings have died or defoliated completely due to accelerated leaf senescence during or just after the
310 treatment period. Since chlorophyll degradation is a common feature of both senescence processes and
311 nutrient remobilization was only measured indirectly by CCI, we did not consider (I) tree saplings that
312 showed an early or abrupt defoliation (without gradual coloration) before the 18th of August (n = 20) and
313 (II) tree saplings with constant CCI values lower than three, the limit at which the values of the CCI meter
314 can be interpreted, for the whole period from August to November (n = 18). Like in other studies, some
315 defoliated tree saplings produced a few new leaves as last attempt to prevent death (Vander Mijnsbrugge
316 et al., 2016;Turcsan et al., 2016). However, there were not enough of such leaves for meaningful analyses.

318 2.4. Statistical analyses

319 All statistical analyses were performed using R v.3.6.1. (R Core Team, 2020). The model assumptions were
320 tested following Zuur et al. (2010). All graphical output is built using the packages R/GGPLOT2, R/GGPUBR,
321 R/VIRIDIS and R/COWPLOT, while data manipulation has been done using R/DPLYR (Wickham, 2009;Wilke,
322 2019;Garnier, 2018;Kassambara, 2019;Wickham et al., 2018).

323

324 2.4.1. Assessing the patterns of CCI and loss of canopy greenness using generalized additive
325 mixed models

326 The patterns of the CCI and loss of canopy greenness data from both our tree saplings and mature trees
327 were assessed using generalized additive mixed models (GAMMs) built using the packages R/MGCV and
328 R/GRATIA (Wood, 2011;Simpson, 2020;Hastie and Tibshirani, 1986;Pedersen et al., 2019). We used GAMMs
329 because they allow more flexibility than other models (e.g. generalized linear models) to model the
330 distribution parameter μ (i.e. the mean of the observed random variable) and the continuous explanatory
331 variables (Rigby and Stasinopoulos, 2005).

332
333 To model the CCI of both our tree saplings and mature trees as a function of their covariates, Gaussian
334 GAMMs with the identity link function were used (Table 2). To model the loss of canopy greenness of both
335 our tree saplings and mature trees as a function of their covariates and because the loss of canopy
336 greenness is scaled between 0 and 1, Binomial GAMMs with the logistic link function were used (Table 2).
337 The GAMMs were chosen with the lowest AIC value (Akaike information criterion) and all factor-smooth
338 interaction terms were smoothed using P-splines to address the large gap in data (i.e. from November to
339 June) between the yearly sampling periods.

340
341 For the CCI of the beech saplings, the fixed covariates were the *treatment* (categorical with three levels),
342 *leaf place* (categorical with three levels) and *day of the year* (continuous; model 1). The interaction term
343 was modelled as a factor-smooth interaction between the covariates *day of the year* and *treatment*. The
344 dependency among observations of the same individual tree was incorporated by using *individual tree* as
345 random intercept.

346 Model 1

$$\begin{aligned} 347 & Y_{ij} \sim \text{Gaussian}(\mu_{ij}, \text{cst.}) \\ 348 & g(\mathbb{E}(Y_{ij})) = g(\mu_{ij}) \\ 349 & g(\mu_{ij}) = \text{Treatment}_{ij} + \text{Leaf place}_{ij} + f(\text{Day of the year}_{ij}, \text{Treatment}_{ij}) + \text{Individual tree}_i \end{aligned}$$

351 where g is the identity link function, μ_{ij} is the conditional mean, Y_{ij} is the j th observation of the response
352 variable (i.e. the CCI) in Individual tree i , and $i = 1, \dots, 128$, and Individual tree $_i$ is the random intercept (Zuur
353 et al., 2007;Zuur et al., 2016).

354 For the loss of canopy greenness of the beech saplings, the fixed covariates were the *treatment*
355 (categorical with three levels) and *day of the year* (continuous; model 2). The interaction term and the
356 dependency among observations of the same individual tree were treated as in model 1.

357 Model 2

$$\begin{aligned} 358 & Y_{ij} \sim \text{B}(n_{ij}, \pi_{ij}) \\ 359 & g(\mathbb{E}(Y_{ij})) = g(\mu_{ij}) \\ 360 & g(\mu_{ij}) = \text{Treatment}_{ij} + f(\text{Day of the year}_{ij}, \text{Treatment}_{ij}) + \text{Individual tree}_i \end{aligned}$$

362 where n_{ij} is the number of observations, π_{ij} is the probability of ‘success’, g is the logit link function, μ_{ij} is
363 the conditional mean, Y_{ij} is the j th observation of the response variable (i.e. the loss of canopy greenness)
364 in Individual tree i , and $i = 1, \dots, 128$, and Individual tree $_i$ is the random intercept.

365 For the CCI of the mature beech, birch and oak trees, the fixed covariates were the *year* (categorical with
366 three levels), *leaf type* (categorical with two levels) and *day of the year* (continuous; model 3). The
367 interaction term was modelled as a factor-smooth interaction between the covariates *day of the*

368 *year* and *Year*. The dependency among observations of the same individual tree was incorporated
369 using *individual tree* as random intercept.

370 Model 3

$$\begin{aligned} 371 & Y_{ij} \sim \text{Gaussian}(\mu_{ij}, \text{cst.}) \\ 372 & g(\mathbb{E}(Y_{ij})) = g(\mu_{ij}) \\ 373 & g(\mu_{ij}) = \text{Year}_{ij} + \text{Leaf type}_{ij} + f(\text{Day of the year}_{ij}, \text{Year}_{ij}) + \text{Individual tree}_i \end{aligned}$$

375 where g is the identity link function, μ_{ij} is the conditional mean, Y_{ij} is the j th observation of the response
376 variable (i.e. the CCI) in Individual tree i , and $i = 1, \dots, 8$ for beech, $i = 1, \dots, 4$ for birch and $i = 1, \dots, 4$ for oak,
377 and Individual tree $_i$ is the random intercept.

378 For the loss of canopy greenness of the mature beech, birch and oak trees, the fixed covariates were the
379 *Year* (categorical with three levels) and *day of the year* (continuous; model 4). The interaction term and
380 the dependency among observations of the same individual tree were treated as in model 3.

381 Model 4

$$\begin{aligned} 382 & Y_{ij} \sim \text{B}(n_{ij}, \pi_{ij}) \\ 383 & g(\mathbb{E}(Y_{ij})) = g(\mu_{ij}) \\ 384 & g(\mu_{ij}) = \text{Year}_{ij} + f(\text{Day of the year}_{ij}, \text{Year}_{ij}) + \text{Individual tree}_i \end{aligned}$$

386 where n_{ij} is the number of observations, π_{ij} is the probability of ‘success’, g is the logit link function, μ_{ij} is
387 the conditional mean, Y_{ij} is the j th observation of the response variable (i.e. the loss of canopy greenness)
388 in Individual tree i , and $i = 1, \dots, 16$ for beech, $i = 1, \dots, 8$ for birch and $i = 1, \dots, 8$ for oak, and Individual
389 tree $_i$ is the random intercept.

390

391 Table 2: Adjusted R², effective degrees of freedom (edf) and F-test values of the GAMM smooth terms
 392 (*Day of the year*). All smooth terms were significant, with p-values < 0.001. $\mathbb{E}(y_i)$ are the expected values
 393 of the response variable y_i , $f(x_i)$ is the smooth function of the covariate x_i , β_i is the intercept of the covariate
 394 x_i , ζ is the random effect and ϵ_i are the errors. All smooth functions were fitted using P-splines. The
 395 chlorophyll content index, loss of canopy greenness, day of the year and tree individual are abbreviated
 396 by CCI, LOCG, Doy and ID, respectively.

397

Site	Species	Y_i	Model equation	Family distribution	Link function	AIC	Adjusted R ²	Smooth term	Treatment	Edf	F or Chi.sq
Wilrijk	<i>Fagus sylvatica</i>	CCI	(1) $g(\mathbb{E}(y_i)) = f_1 \text{Treatment}_i(Doy) + \beta_1 \text{Treatment}_i + \beta_2 \text{Leaf_place}_i + \zeta_{ID} + \epsilon_i$	Gaussian	Identity	17373	0.61	Day of the year	Reference	4.8	337.5
									+0 °C	5.8	175
									+3 °C	6.1	34.4
Wilrijk	<i>Fagus sylvatica</i>	Loss of canopy greenness	(2) $g(\mathbb{E}(y_i)) = f_1 \text{Treatment}_i(Doy) + \beta_1 \text{Treatment}_i + \zeta_{ID} + \epsilon_i$	Binomial	Logit	878	0.76	Day of the year	Reference	3.6	112.6
									+0 °C	1.1	105.9
									+3 °C	1	53.7
KS & PB	<i>Fagus sylvatica</i>	CCI	(3) $g(\mathbb{E}(y_i)) = f_1 \text{Year}(Doy) + \beta_1 \text{Year} + \beta_2 \text{Leaf_type}_i + \zeta_{ID} + \epsilon_i$	Gaussian	Identity	9382	0.7	Day of the year	2017	4.6	197.8
									2018	5.3	221.6
									2019	5.2	193.2
KS & PB	<i>Fagus sylvatica</i>	Loss of canopy greenness	(4) $g(\mathbb{E}(y_i)) = f_1 \text{Year}(Doy) + \beta_1 \text{Year} + \zeta_{ID} + \epsilon_i$	Binomial	Logit	450	0.87	Day of the year	2017	2.4	44.8
									2018	2.5	70.6
									2019	2.7	66
KS	<i>Betula pendula</i>	CCI	(5) $g(\mathbb{E}(y_i)) = f_1 \text{Year}(Doy) + \beta_1 \text{Year} + \beta_2 \text{Leaf_type}_i + \zeta_{ID} + \epsilon_i$	Gaussian	Identity	4546	0.44	Day of the year	2017	3.2	25.9
									2018	5	56.9
									2019	3.1	14.7
KS	<i>Betula pendula</i>	Loss of canopy greenness	(6) $g(\mathbb{E}(y_i)) = f_1 \text{Year}(Doy) + \beta_1 \text{Year} + \zeta_{ID} + \epsilon_i$	Binomial	Logit	254	0.89	Day of the year	2017	1	20.6
									2018	1	36
									2019	1.6	48.2
PB	<i>Quercus robur</i>	CCI	(7) $g(\mathbb{E}(y_i)) = f_1 \text{Year}(Doy) + \beta_1 \text{Year} + \beta_2 \text{Leaf_type}_i + \zeta_{ID} + \epsilon_i$	Gaussian	Identity	5694	0.52	Day of the year	2017	3.3	62.5
									2018	5.1	84.4
									2019	4.3	30.7
PB	<i>Quercus robur</i>	Loss of canopy greenness	(8) $g(\mathbb{E}(y_i)) = f_1 \text{Year}(Doy) + \beta_1 \text{Year} + \zeta_{ID} + \epsilon_i$	Binomial	Logit	225	0.85	Day of the year	2017	1.2	12.5
									2018	1.9	33.6
									2019	2.4	32

398

399 2.4.2. Using breakpoints to indicate the onset of autumn leaf senescence and the onset of the
400 loss of canopy greenness

401 In principle, the onset of autumn leaf senescence could be derived from the CCI or loss of canopy
402 greenness. However, Mariën et al. (2019) recently showed that the latter method cannot be used under
403 severe drought stress. Therefore, two phenological variables were considered to describe the autumn
404 canopy dynamics: the onset of autumn leaf senescence derived from the CCI (the onset of autumn leaf
405 senescence) and the onset of the loss of canopy greenness. For each tree, we defined the onset of autumn
406 leaf senescence and the onset of loss of canopy greenness as the date by which the variable of interest
407 started to decline substantially in early autumn. These dates were calculated using piecewise linear
408 regressions and are represented by the breakpoints resulting from these analyses (Menzel et al.,
409 2015; Mariën et al., 2019; Xie and Wilson, 2020). The piecewise linear regressions were performed using
410 R/SEGMENTED (Vito and Muggeo, 2008). The uncertainty reported represents the inter-tree variability.
411 Trees that did not show a clear breakpoint (13 in the manipulative experiment) were not considered in
412 the analysis. These trees did not show a different pattern of CCI or loss of canopy greenness than the
413 other trees (Fig. A2).

414
415 2.4.3. Comparing the onset of autumn leaf senescence among tree saplings exposed to different
416 treatments

417 We tested whether the beech saplings exposed to the three treatments in 2018 differed in their onset of
418 autumn leaf senescence using a linear model with the onset of autumn leaf senescence as response
419 variable and *treatment* (categorical with three levels) as fixed covariate. The residuals of the model were
420 approximately normally distributed and a Breusch-Pagan test, the R/ncvTest and R/bptest in the R/CAR and
421 R/LMTEST packages, showed no evidence of heteroscedasticity ($P > 0.05$) (Fox and Weisberg, 2019; Zeileis
422 and Hothorn, 2002). A one-way ANOVA was used to detect significant differences in the onset of autumn
423 leaf senescence among the treatments.

424
425 2.4.4. Comparing the onset of autumn leaf senescence and the onset of loss of canopy greenness
426 in mature trees among species and years

427 To model the onset of autumn leaf senescence and the onset of the loss of canopy greenness as a function
428 of their covariates, Gaussian linear mixed models were used. These models were built with the package
429 R/LME4 (Bates et al., 2015).

430
431 The effect of the year on the onset of autumn leaf senescence and the onset of the loss of canopy
432 greenness was assessed using two linear mixed effect models with the onset of autumn leaf senescence
433 and the onset of the loss of canopy greenness from the mature beech, birch and oak trees as response
434 variable. The fixed covariate in these two models was the *Year* (categorical with three levels; model 5). To
435 incorporate the dependency among observations of the same species, we used *species* as random
436 intercept.

437 Model 5

438
$$Y_{ij} \sim \text{Gaussian}(\mu_{ij}, \text{cst.})$$

439
$$g(\mathbb{E}(Y_{ij})) = g(\mu_{ij})$$

440
$$\mu_{ij} = \text{Year}_{ij} + \text{Species}_i$$

441

442 where g is the identity link function, μ_{ij} is the conditional mean, Y_{ij} is the j th observation of the response
443 variable in Species i , and $i = 1, \dots, 3$ and Species_i is the random intercept.

444 The effect of the species on the onset of autumn leaf senescence and the onset of the loss of canopy
445 greenness was assessed using two linear mixed effect models with the onset of autumn leaf senescence
446 and the onset of the loss of canopy greenness from the mature beech, birch and oak trees as response
447 variable. The fixed covariate in these two models was the *Species* (categorical with three levels; model 6).
448 To incorporate the dependency among observations of the same year, we used *Year* as random intercept.

449 Model 6

$$\begin{aligned} 450 & Y_{ij} \sim \text{Gaussian}(\mu_{ij}, \text{cst.}) \\ 451 & g(\mathbb{E}(Y_{ij})) = g(\mu_{ij}) \\ 452 & \mu_{ij} = \text{Species}_j + \text{Year}_i \end{aligned}$$

454 where g is the identity link function, μ_{ij} is the conditional mean, Y_{ij} is the j th observation of the response
455 variable in Year i , and $i = 1, \dots, 3$ and Year_i is the random intercept.

456 The residuals of the models were approximately normally distributed and showed no heteroscedasticity
457 (tested using diagnostic plots). Therefore, we used Pearson's chi-square test, $R/\text{drop1}$ in the $R/\text{LME4}$
458 package, to detect significant differences in the onset of autumn leaf senescence and the onset of the loss
459 of canopy greenness among the predictor variables. A multiple comparison test, the R/glht test with
460 method Tukey in the $R/\text{MULTCOMP}$ package, was used to test for significant differences among the means
461 of the levels in the predictor variables (Hothorn et al., 2008).

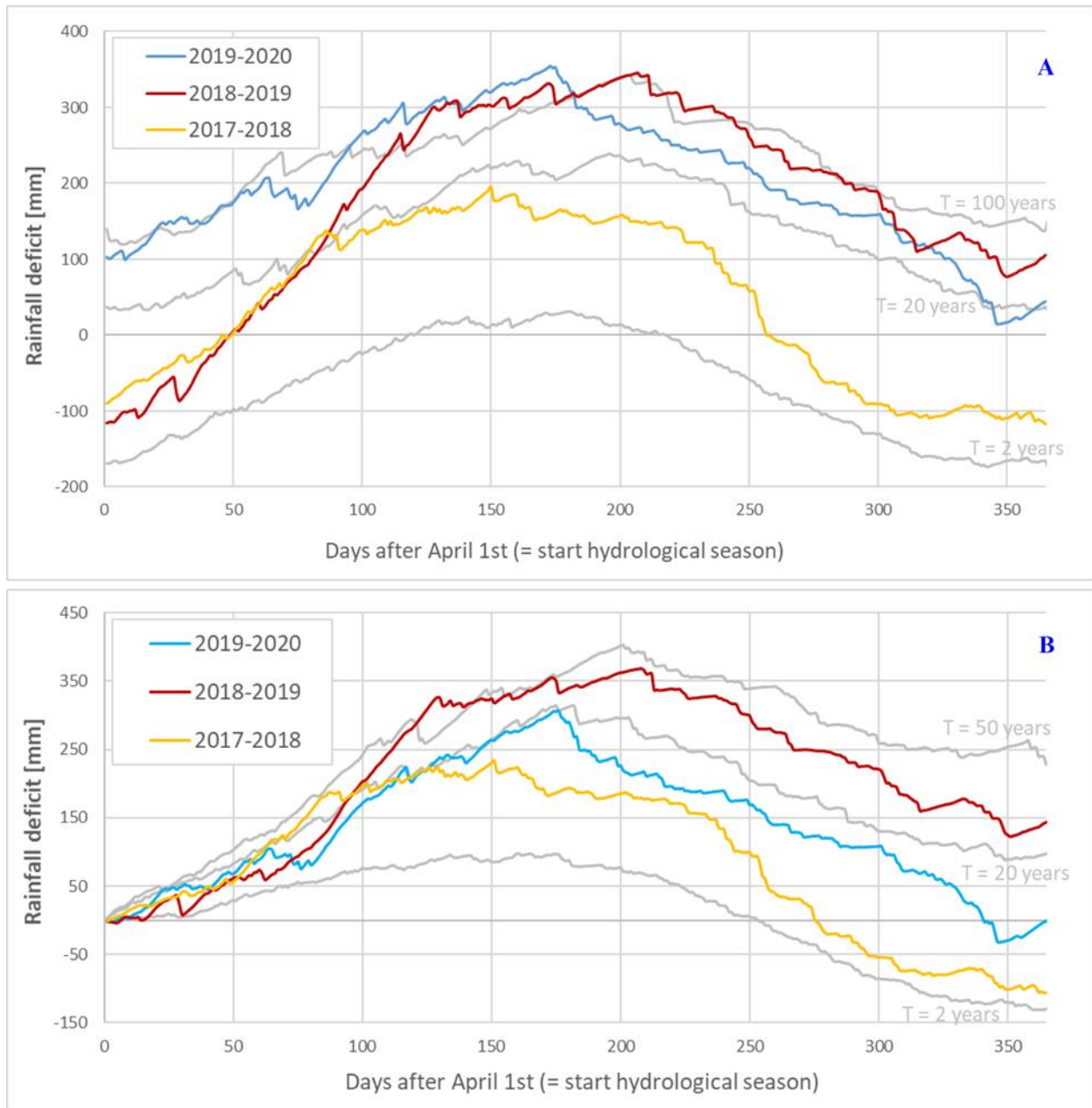
462 3. Results

463 3.1. Magnitude of the drought stress in 2017, 2018 and 2019

464 The weather in 2018 and 2019 was exceptional, as can be seen in the overview of the meteorological
465 conditions from 2017 to 2019 against the long-term reference values in Table 1 and Figure 2. In 2017, the
466 weather during spring was dry and warm but the weather during summer and autumn was relatively
467 normal (KMI, 2017b, c, a). In contrast, the warm and dry summer of 2018 was marked by abnormal (with
468 an average return time of 6 years) to exceptional (with an average return time of 30 years or more) values
469 (KMI, 2018b). Furthermore, the autumn of 2018 was abnormally dry and all precipitation fell on relatively
470 few days (32) (KMI, 2018a). In the summer of 2019, the average air temperature and the total amount of
471 sunshine were both among the three highest values recorded since 1981. In fact, the absolute maximum
472 air temperature record for Belgium was broken in 2019 (KMI, 2019b). On the other hand, the autumn of
473 2019 was considered normal (KMI, 2019a).

474
475 The rainfall deficit for each day in the hydrological year (from the 1st of April until the 31st of March) and
476 different return times are shown in Figure 3 (panel A & B). This demonstrates that in the late spring of
477 2017, the summer of 2018 and the summer of 2019 the rainfall deficit reached a return time between 20
478 and 50 years, 50 years, and 20 years, respectively. The hydrological summers of 2017, 2018 and 2019 had
479 therefore moderate to extremely dry conditions, which led to accumulated rainfall deficit conditions over
480 time (see Figure 3; panel A). Especially the hydrological year starting in 2018 ended with a strong rainfall
481 deficit of about 150 mm, which was not reduced during 2019. The effects of this strong rainfall deficit are
482 also apparent in the lower volumetric soil water content values (ca. 5% less) measured at the beginning
483 of 2019, compared to the same measurements in 2017 and 2018.

484



485

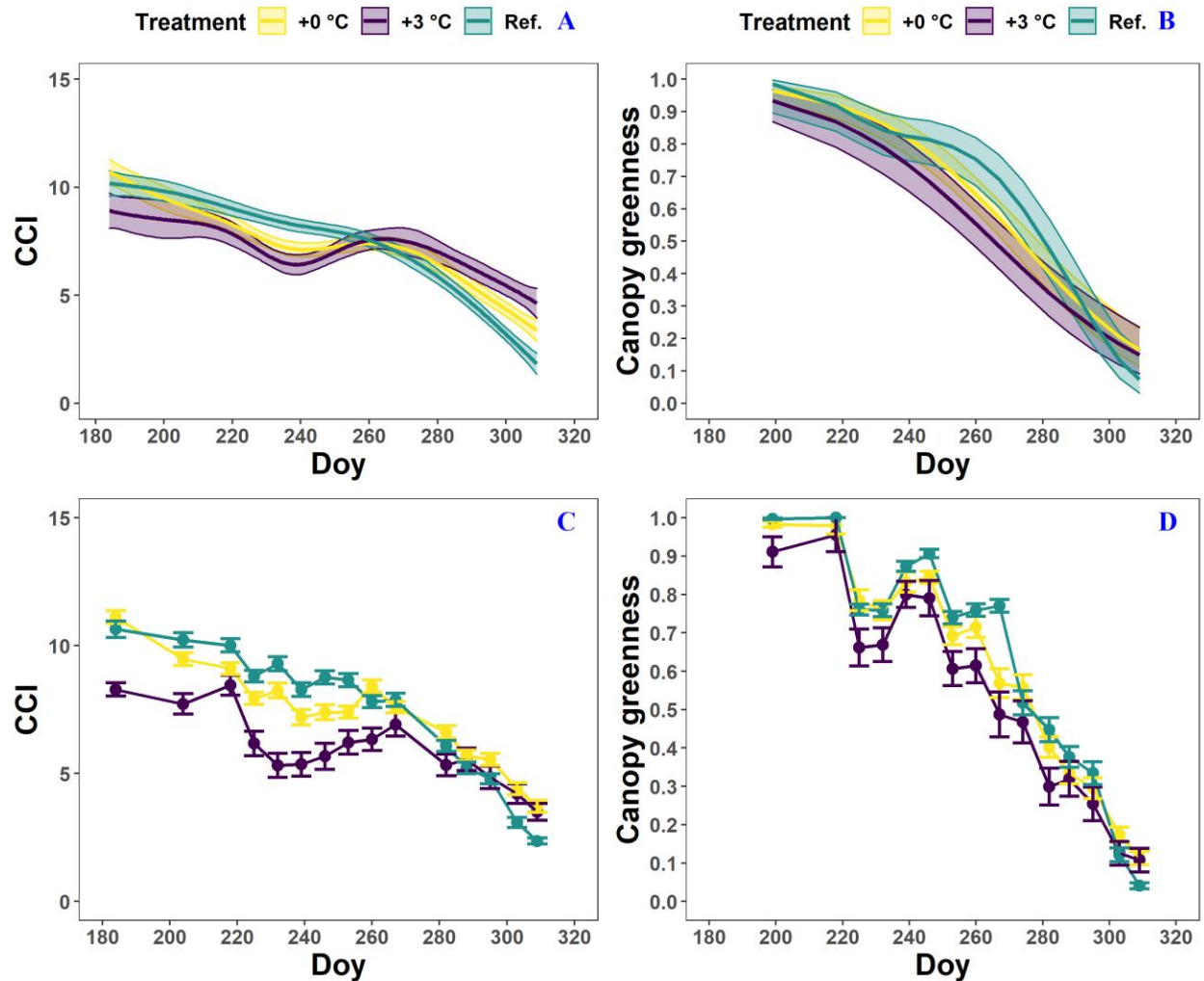
486 Fig. 3: The rainfall deficit for the meteorological station of the Royal Meteorological Institute (KMI) in
 487 Ukkel, Belgium. The colored solid lines represent the rainfall deficit for the hydrological years in the period
 488 2017-2020, while the grey solid lines represent the long-term reference statistics (computed for the 100-
 489 year period 1901 - 2000) with T as the return period, which represents the mean time between two
 490 successive exceedances of a given deficit value and is computed in an empirical way (Willems, 2000, 2013).
 491 Panel A uses a continuous computation, while panel B starts from a zero deficit on the first of April (the
 492 start of the hydrological year). The colors represent the rainfall deficit in 2017 (light blue), 2018 (red) and
 493 2019 (yellow).
 494

495 3.2. The effect of drought, heat stress and increased atmospheric aridity on the onset of autumn
496 leaf senescence in tree saplings in the manipulative experiment

497 For all treatments, the CCI values of the beech saplings showed an overall moderate decrease until the
498 beginning of October. Afterwards, this decrease accelerated (Fig. 4; panel A & C; Table 2). In the +0 °C and
499 especially the +3 °C treatment, an abnormal CCI decline was observed in early August with only a partial
500 recovery later on. As a result, from the beginning of August until mid-September, the CCI values of the
501 beech saplings in the reference plots were significantly higher than the CCI values of the beech saplings in
502 the glasshouses. From the end of September, the CCI decreased in all treatments, showing similar CCI
503 measurements across treatments. However, the modeled CCI of the +3 °C treatment declined slower than
504 the modeled CCI of the other two treatments. No significant difference was detected in the timing of the
505 onset of autumn leaf senescence among the beech saplings exposed to the three different treatments, as
506 the mean onset of autumn leaf senescence was between the 21st (DOY = 260 ± 5) and 25th (DOY = 264 ±
507 4) of September ($P = 0.7$; Fig. A3).

508
509 The canopy greenness for the beech saplings showed a stable decline from early August until the end of
510 autumn (Fig. 4; panel B & D; Table 2). Nevertheless, during September, the canopy greenness of the beech
511 saplings in the reference plots was significantly higher than the canopy greenness of the beech saplings in
512 the glasshouses with the +3 °C treatment.

513
514 The tree saplings in the glasshouses of both treatments were exposed to a high mortality with 14% and
515 26% of the tree saplings in the glasshouses with the +0 °C and +3 °C treatment, respectively, considered
516 'dead' along our criteria (see §2.3.). In the reference plots, no beech saplings died.



517

518 Fig. 4: The generalized additive mixed model fits for the chlorophyll content index (CCI; panel A) and loss
 519 of canopy greenness (panel B) of the *Fagus sylvatica* saplings at the Drie Eiken Campus in Wilrijk. The
 520 colored solid lines represent smooth terms, while the colored shaded bands around the smooth terms
 521 approximate the 95% simultaneous confidence intervals (panel A) and 95% pointwise confidence intervals
 522 (panel B). The dots and error bars represent the mean CCI (panel C) and mean canopy greenness (panel
 523 D) with standard errors. The colors represent the CCI or the loss of canopy greenness of the beech saplings
 524 in the reference plots (green; Ref.), the glasshouses that followed the outside ambient air temperature
 525 (yellow; +0 °C) and the glasshouses that were three degrees warmer than the outside ambient air
 526 temperature (purple; +3 °C), respectively.

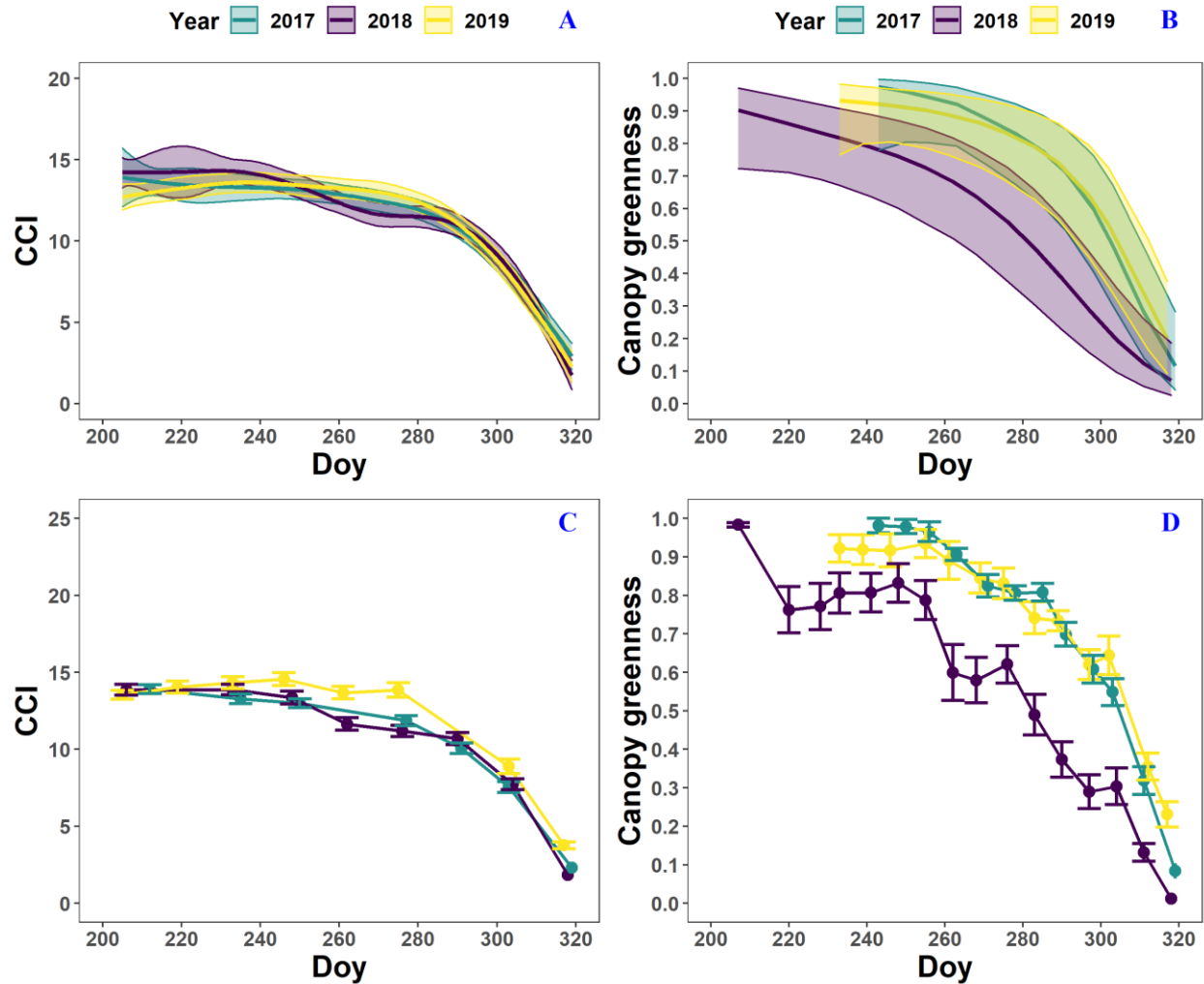
527

528 3.3. Inter-annual and inter-species variability in the timing of the onset of autumn leaf senescence
529 and the onset of the loss of canopy greenness in mature trees

530 The pattern in the CCI values for the mature beech, birch and oak trees seems consistent throughout the
531 years with stable values in summer and a rapid decline around late October (Fig. 5 - 7; panel A & C; Table
532 2). We also observed no significant difference in the onset of autumn leaf senescence among the years (P
533 = 0.09) and species ($P = 1$). The mean onset of autumn leaf senescence among the years was from the 8th
534 (DOY = 281 ± 6) to the 19th (DOY = 292 ± 6) of October (Fig. A4; panel A), while the mean onset of autumn
535 leaf senescence among the species was around the 13th of October (DOY = 286 ± 6; Fig. A4; panel B). The
536 CCI correlated linearly with the chlorophyll concentrations but the data showed more variation in 2018
537 than 2017 (see Fig. A1).

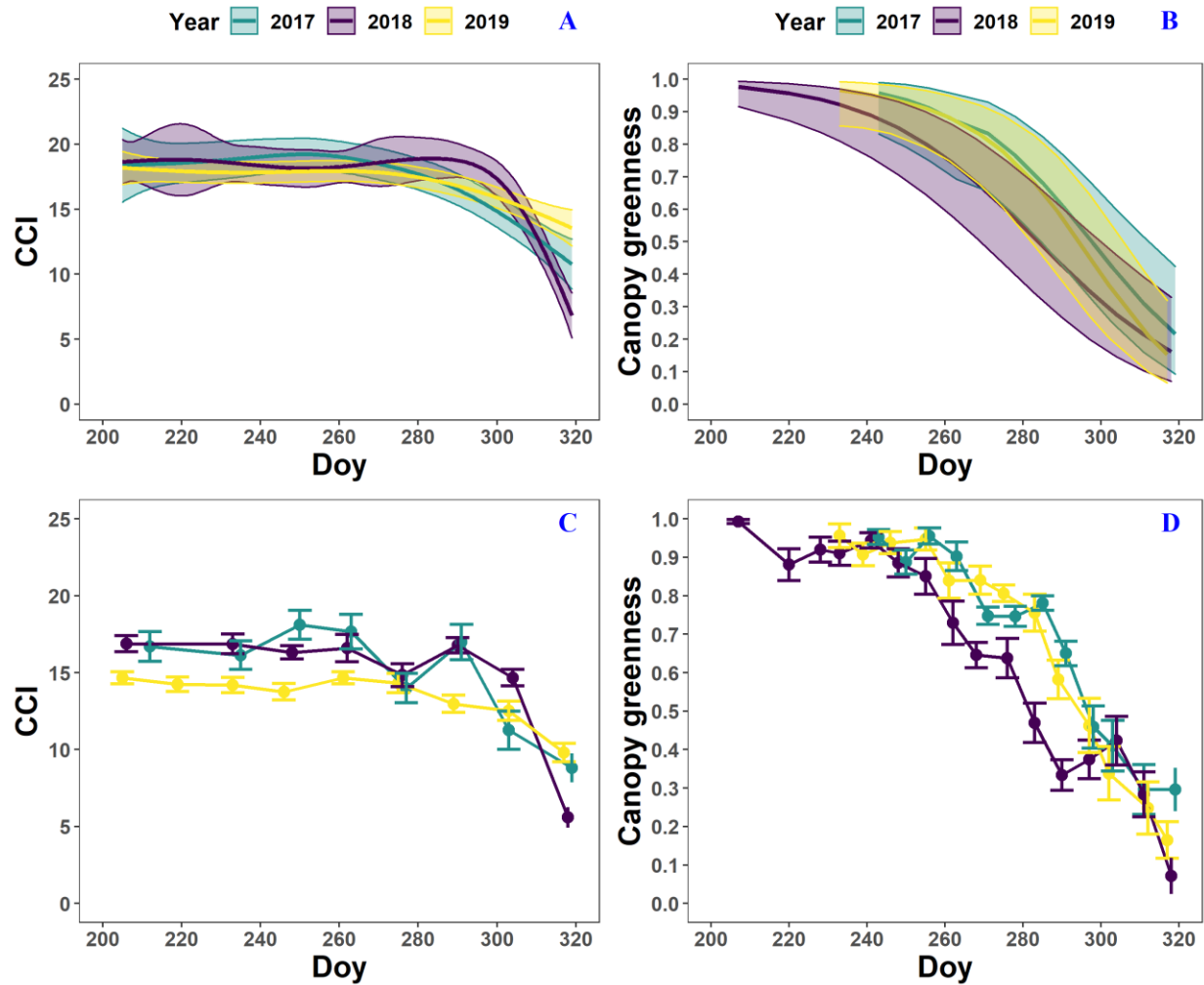
538
539 The pattern in the canopy greenness for the mature beech, birch and oak trees seemed less consistent
540 throughout the years (Fig. 5 - 7; panel B & D; Table 2). The loss of canopy greenness showed a very similar
541 pattern between 2017 and 2019 for birch and beech, with the start of the decline in canopy greenness
542 values around late September for birch and late October for beech. Like beech and birch, oak showed a
543 standard pattern in 2019 with the start of the seasonal decline in late October. However, in 2017, oak
544 showed an earlier loss of canopy greenness with the start of the seasonal decline in mid-September. In all
545 cases, a rapid decline in the canopy greenness was observed in late autumn. In 2018, all species showed
546 an earlier and steeper decline in their canopy greenness values. This effect was also reflected by a
547 significant difference in the onset of the loss of canopy greenness among the years ($P = 5 \times 10^{-11}$). Across
548 species, the onset of the loss of canopy greenness did not differ significantly ($P = 0.9$) between 2017 (DOY
549 = 292 ± 9) and 2019 (DOY = 290 ± 4), while it occurred 26 and 25 days earlier in 2018 (DOY = 266 ± 4)
550 compared to 2017 ($P = 1 \times 10^{-5}$) and 2019 ($P = 1 \times 10^{-5}$), respectively (Fig. A5; panel A). However, all tree
551 species differed significantly in their onset of the loss of canopy greenness across years ($P = 6 \times 10^{-9}$).
552 Compared to birch (DOY = 268 ± 9; Fig. A5; panel B), the onset of the loss of canopy greenness for beech
553 was on average 16 days later ($P = 1 \times 10^{-4}$; DOY = 284 ± 4), while for oak this was 30 days later ($P = 1 \times 10^{-4}$;
554 DOY = 298 ± 4). The onset of the loss of canopy greenness for beech was also 14 days earlier than that
555 for oak ($P = 7 \times 10^{-4}$).

556

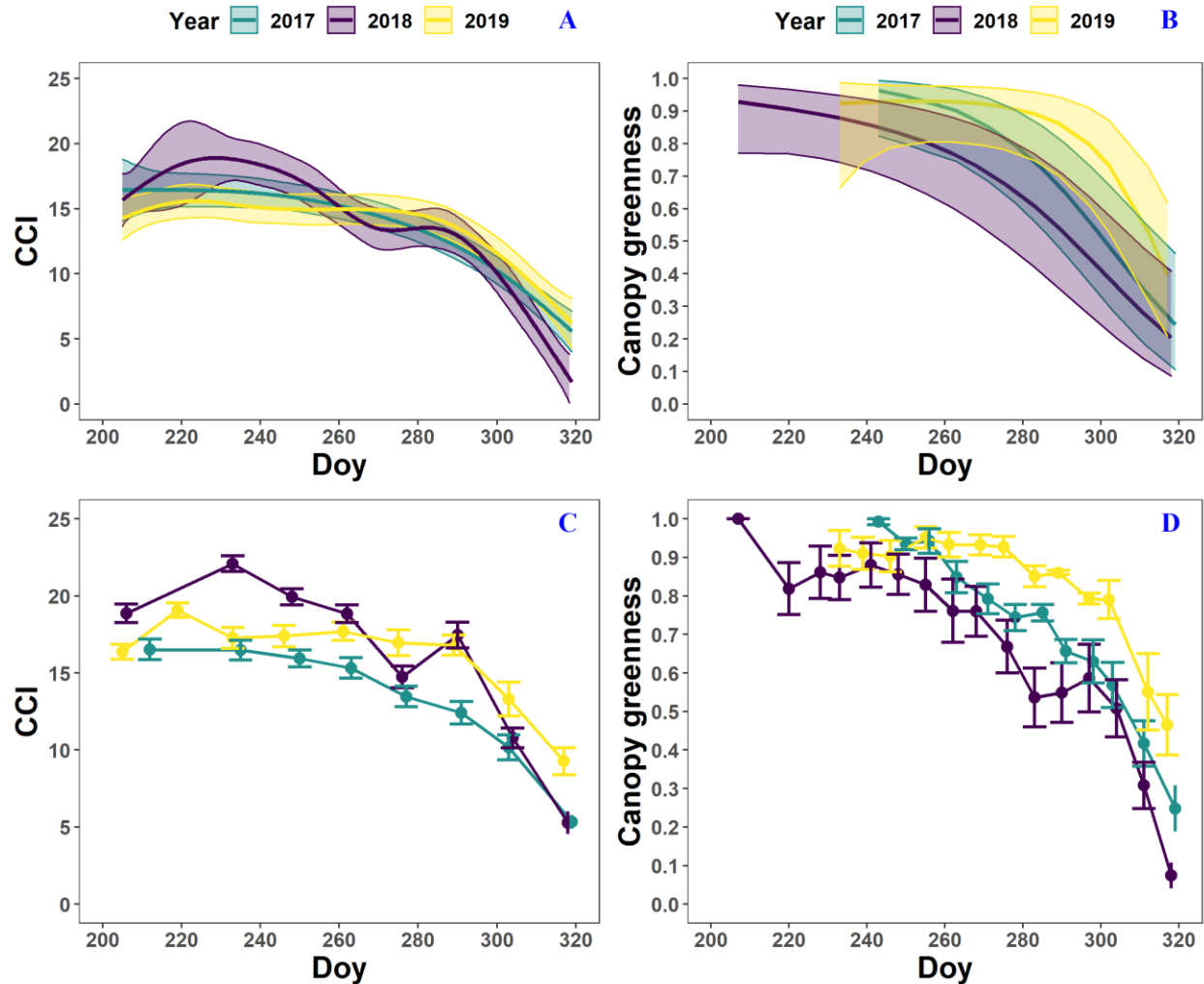


557

558 Fig. 5: The generalized additive mixed model fits for the chlorophyll content index (CCI; $n = 8$; panel A) and
 559 loss of canopy greenness ($n = 16$; panel B) of the mature *Fagus sylvatica* trees at the Klein Schietveld and
 560 Park of Brasschaat. The colored solid lines represent smooth terms, while the colored shaded bands
 561 around the smooth terms represent approximate 95% simultaneous confidence intervals (panel A) and
 562 95% pointwise confidence intervals (panel B). The dots and error bars represent the mean CCI (panel C)
 563 and mean canopy greenness (panel D) with standard errors. The colors represent the CCI or the loss of
 564 canopy greenness of the mature beech trees in 2017 (green), 2018 (purple) and 2019 (yellow).
 565



566
 567 Fig. 6: The generalized additive mixed model fits for the chlorophyll content index (CCI; $n = 4$; panel A) and
 568 loss of canopy greenness ($n = 8$; panel B) of the mature *Betula pendula* trees at the Klein Schietveld. The
 569 colored solid lines represent smooth terms, while the colored shaded bands around the smooth terms
 570 represent approximate 95% simultaneous confidence intervals (panel A) and 95 % pointwise confidence
 571 intervals (panel B). The dots and error bars represent the mean CCI (panel C) and mean canopy greenness
 572 (panel D) with standard errors. The colors represent the CCI or the loss of canopy greenness of the mature
 573 birch trees in 2017 (green), 2018 (purple) and 2019 (yellow).
 574



575
 576 Fig. 7: The generalized additive mixed model fits for the chlorophyll content index (CCI; $n = 4$; panel A) and
 577 loss of canopy greenness ($n = 8$; panel B) of the mature *Quercus robur* trees at the Park of Brasschaat. The
 578 colored solid lines represent smooth terms, while the colored shaded bands around the smooth terms
 579 represent approximate 95% simultaneous confidence intervals (panel A) and 95% pointwise confidence
 580 intervals (panel B). The dots and error bars represent the mean CCI (panel C) and mean canopy greenness
 581 (panel D) with standard errors. The colors represent the CCI or the loss of canopy greenness of the mature
 582 oak trees in 2017 (green), 2018 (purple) and 2019 (yellow).
 583

584 4. Discussion

585 Our results showed that the timing of the onset of autumn leaf senescence in both tree saplings and
586 mature trees was not significantly altered by severe drought, heat stress and increased atmospheric
587 aridity induced by a decline in the soil moisture, relative humidity, and an increase in the air temperature
588 and vapor pressure deficit. These results are in contrast to other studies reporting, for example, that
589 drought stress delays the onset of autumn leaf senescence (determined using remote sensing indices or
590 visual assessment) (Wang et al., 2016;Vander Mijnsbrugge et al., 2016;Zeng et al., 2011;Gárate-Escamilla
591 et al., 2020;Seyednasrollah et al., 2020). However, in our study, drought, heat stress and increased
592 atmospheric aridity did affect the loss of CCI and canopy greenness of our beech saplings, their mortality,
593 and the onset of the loss of canopy greenness in our mature trees. The effect of the drought, heat stress
594 and increased atmospheric aridity on the loss of canopy greenness might be due to an early leaf abscission
595 in response to hydraulic failure of the branches (Wolfe et al., 2016;Munné-Bosch and Alegre, 2004). The
596 manipulation experiment on the beech saplings also revealed that the 'drought/less irrigation' treatment
597 alone (the + 0°C treatment) had less impact (e.g. lower tree mortality, lower premature degradation of
598 chlorophyll in summer) than the combined 'drought/less irrigation, warming and increased atmospheric
599 aridity' treatment (the + 3°C treatment). The decline in the CCI of the saplings exposed to the +3°C
600 treatment, around mid-August, might indicate that physiological damage due to stress can accumulate
601 and become apparent even though stress is alleviated.

602
603 Our experimental design did not allow disentangling the effect of the three different stressors within the
604 + 3°C treatment (i.e. drought/less irrigation, warming and increased atmospheric aridity). However, Fu et
605 al. (2018) found that summer warming delayed senescence in beech. In addition, Kint et al. (2012) found
606 that growth in beech is primarily controlled by the water deficit and low relative humidity values during
607 summer. Therefore, the effects observed in the + 3°C treatment might be mainly related to the
608 atmospheric aridity. For the mature trees, the different drought response of the autumn pattern of
609 chlorophyll (no effect) and the loss of canopy greenness (advanced and enhanced) is probably an
610 important reason of confusion still present today in the literature on the relationship between drought
611 and autumn senescence. While the detoxification of chlorophyll is a prerequisite for the expression of
612 different coloration values, chlorophyll does not degrade at the same speed as other leaf pigments. In
613 fact, not even all leaf pigments degrade (or are formed) at the same velocity throughout the senescence
614 process (Keskitalo et al., 2005). Consequently, observations of changing coloration levels are difficult to
615 interpret. Moreover, note that coloration measurements also take into account leaf yellowing and
616 mortality due to hydraulic failure.

617
618 The continuously computed rainfall deficit was similar between 2018 and 2019. Nevertheless, the loss of
619 canopy greenness suggests that the drought of 2019, which coincided with several heat waves and
620 increased atmospheric aridity, might have been less damaging for the late-summer leaf dynamics than
621 the drought of 2018 (which lasted longer). The rainfall deficit starting from a zero deficit supports the
622 observation that, despite the accumulated drought effect, the drought of 2019 was less severe in the
623 growing season than the drought of 2018. Perhaps, the conditions of 2018 (i.e. sunny and warm with high
624 vapor pressure deficits, and a long period with a low soil moisture starting earlier than in 2019) triggered
625 the damaging process of cavitation in the trees, while this might have occurred less intensively in 2019 if
626 the stomatal conductance was lower (Barigah et al., 2013;Bolte et al., 2016;Banks et al., 2019).
627 Alternatively, the difference in the timing of the drought peaks (i.e. the drought of 2018 peaked around
628 one month and half earlier than the drought of 2019, Fig. 3A) could have led to divergent responses due
629 to differences in drought sensitivity along the growing season (Banks et al., 2019).

630

631 The drought (but also the heat stress and increased atmospheric aridity) did not affect the onset of
632 autumn leaf senescence of both the beech saplings and the mature trees. Deciduous trees therefore seem
633 to have a conservative strategy concerning the timing of their autumn leaf senescence that might be under
634 the control of a constant variable (e.g. the day-length or spectral quality) (Michelson et al., 2018;Chiang
635 et al., 2019). Such a strategy prioritizes carbon uptake over nutrient remobilization, as a fixed onset of
636 autumn leaf senescence would not allow an advanced nutrient remobilization when required (Keskitalo
637 et al., 2005;Brelsford et al., 2019). Moreover, such a strategy makes the trees vulnerable against the
638 effects of early frost. In case of early frost, the trees might not complete their nutrient resorption. Possible
639 consequences of an incomplete nutrient resorption over a longer time period might include a decline in
640 the overall fitness of the trees and negative feedbacks on the growth dynamics of the next season, such
641 as less buds (Fu et al., 2014;Vander Mijnsbrugge et al., 2016;Crabbe et al., 2016). Although Fu et al. (2014)
642 suggested a correlation between the bud burst and the onset of autumn leaf senescence, we have found
643 no relationships for 2018 and 2019 in birch and beech, but a positive relationship in oak (every delay of
644 one day in the bud burst corresponded to a delay of \pm two days in the onset of autumn leaf senescence).

645
646 Surprisingly, the onset of autumn leaf senescence did not differ significantly among the different tree
647 species, which supports the idea that the onset of autumn leaf senescence in different deciduous trees
648 might be controlled by the same (light related) signal. Perhaps the onset of leaf senescence is timed in a
649 manner similar to flowering, as put forward by the external coincidence model (i.e. clock-regulated gene
650 expression and light both determine the perception of photoperiodism) (Böhlenius et al., 2006;Kobayashi
651 and Weigel, 2007;Koornneef et al., 1991;Yanovsky and Kay, 2002). Other explanations for the lack of
652 significant differences in the onset of autumn leaf senescence among the species could have been the
653 small sample size (i.e. eight beech, four birch and four oak trees for the CCI measurements) or the
654 inaccuracies related to the method of piece-wise linear regressions. Given our results, the drought in 2017,
655 2018 and 2019 had little impact on the CCI trend and onset of autumn leaf senescence in mature beech,
656 birch and oak trees.

657
658 In this regard, the exact impact of the light quantity and spectral quality on the trigger for the onset of
659 senescence (directly or indirectly through photoperiodic detection), is not well known in deciduous trees
660 (Michelson et al., 2018). If phytochrome only responds to the presence of red wavelengths, the effect of
661 the polycarbonate in the glasshouses must have been minimal. However, experimental biases might be
662 caused if cryptochrome, which is sensitive to UV light and active at low fluency rates, played a significant
663 role in the onset of senescence (Schulze et al., 2019;Smith, 1982). Because very low light intensities are
664 required by plants to generate a photosynthetic potential (a minimum scalar irradiance of $\pm 1 \mu\text{mol}/\text{m}^2$)
665 and very low fluencies (starting from $0.1 \mu\text{mol}/\text{m}^2$) are required for phytochrome action, we assumed the
666 decrease in the incoming light intensity would not have had a significant effect (Legris et al., 2019;Poorter
667 et al., 2019;Franklin and Quail, 2010;Legris et al., 2016;Neff et al., 2000;Mancinelli and Rabino, 1978).

668
669 Although the onset of autumn leaf senescence in both the tree saplings and the mature trees was not
670 advanced by drought, heat stress and increased atmospheric aridity, the onset of autumn leaf senescence
671 in beech saplings was around 22 days earlier than mature beech trees. Such difference could be due to
672 the different growing conditions (pots versus normal soil), environmental conditions at the different sites,
673 the difference in the average leaf age (tree saplings have an earlier bud-burst than mature trees) or the
674 different ecophysiological response of tree saplings and mature trees (e.g. tree saplings are more
675 vulnerable than mature trees and therefore are likely to use different functional strategies) (Niinemets,
676 2010;Vander Mijnsbrugge et al., 2016;Pšidová et al., 2015). As there is very little difference in the light
677 conditions among the different sites, the difference in the day length is unlikely to have affected the
678 difference in the timing of the onset of autumn leaf senescence between the beech saplings and mature

679 trees. However, it is possible that the beech saplings have a different sensitivity to the light cues, as they
680 usually grow in the understory and therefore under a different light regime than mature trees (Brelsford
681 et al., 2019;Michelson et al., 2018;Chiang et al., 2019).

682
683 Concerning the onset of the loss of canopy greenness for all species and opposed to 2017 (i.e. a year with
684 normal environmental conditions in late-summer and autumn) and 2019 (i.e. a year with high
685 temperatures in summer, relatively normal precipitation in summer and autumn, but suffering from the
686 accumulated effects of the rainfall deficit), the onset of the loss of canopy greenness in 2018 was around
687 three-and-a-half weeks earlier. The canopy greenness metric had been declining earlier in 2018 because
688 the leaves have likely been shed earlier due to an advanced leaf abscission process to protect the tree
689 from hydraulic failure (Munné-Bosch and Alegre, 2004;Wolfe et al., 2016). There was also a difference in
690 the onset of the loss of canopy greenness among the species. This might be due to two reasons. First,
691 birch (the species with the earliest onset of the loss of canopy greenness) has an indeterministic growth
692 pattern, which also means continuous leaf mortality. Second, the fact that oak (the species with the latest
693 onset of the loss of canopy greenness) has typically a second leaf flush, which might connect the difference
694 between beech and oak to differences in leaf longevity.

695
696 Overall, the GAMMs reproduced reliable fits of the CCI and canopy greenness. One of the few observed
697 issues was a small mismatch between the mean CCI shown by the smoother of the fitted GAMM and the
698 mean CCI shown by the line plot for the + 3°C treatment at the end of the growing season (early October
699 – mid November). The overestimation of the CCI in this case might reflect the limitations of using Gaussian
700 GAMMs here

701 5. Conclusion

702 The different environmental conditions of three years (comprising a severe dry year and a severe warm
703 year) did not affect the timing of the onset of autumn leaf senescence in mature beech, birch and oak
704 forest trees in Belgium. This suggests that deciduous trees have a conservative strategy concerning the
705 timing of their senescence. Like our mature beech trees, beech saplings exposed to drought, heat stress
706 and increased atmospheric aridity also did not show any advancement in their onset of autumn leaf
707 senescence compared to beech saplings in normal conditions. Although the drought, heat stress and
708 increased atmospheric aridity did not affect the timing of the onset of autumn leaf senescence, it is clear
709 from our results that they affect the mortality rate in tree saplings and the leaf mortality in mature trees.

710 Data availability

711 The code and data corresponding to the work presented in this article is available at Zenodo as doi:
712 10.5281/zenodo.4559535

713 Author contributions

714 MC and HDB designed the experiment. ID, SL, PW and BM collected the data. PW computed the rainfall
715 deficit, while BM performed all other analyses. BM, PW and MC wrote the text. All authors contributed to
716 the discussions.

717 Competing interests

718 The authors declare that they have no conflict of interest.

719 Acknowledgements

720 The authors acknowledge the funding provided by the ERC Starting Grant LEAF-FALL (714916) and the
721 DOCPRO4 fellowship provided to BM by the University of Antwerp. We also express our gratitude to the
722 Flemish Institute for Nature and Forest (INBO), the Integrated Carbon Observation System (ICOS), the
723 Belgian Royal Meteorological Institute (KMI) and the Royal Dutch Meteorological Institute (KNMI) for
724 providing meteorological data. We would also thank the Agency for Forest and Nature of the Flemish
725 Government (ANB), the Belgian Armed Forces and the Municipality of Brasschaat because they gave
726 permission to conduct research in the study areas. Special thanks are due to Dirk Leyssens (ANB) and
727 Bergen boomverzorging.

728 References

- 729 Banks, J. M., Percival, G. C., and Rose, G.: Variations in seasonal drought tolerance rankings, *Trees*, 33,
730 1063-1072, 10.1007/s00468-019-01842-5, 2019.
- 731 Barigah, T. S., Charrier, O., Douris, M., Bonhomme, M., Herbette, S., Ameglio, T., Fichot, R., Brignolas, F.,
732 and Cochard, H.: Water stress-induced xylem hydraulic failure is a causal factor of tree mortality in
733 beech and poplar, *Ann. Bot.*, 112, 1431-1437, 10.1093/aob/mct204, 2013.
- 734 Bates, D., Mächler, M., Bolker, B., and Walker, S.: Fitting Linear Mixed-Effects Models Using lme4, *Journal*
735 *of Statistical Software*, 67, 1-48, 10.18637/jss.v067.i01, 2015.
- 736 Benbella, M., and Paulsen, G. M.: Efficacy of Treatments for Delaying Senescence of Wheat Leaves: II.
737 Senescence and Grain Yield under Field Conditions, *Agron. J.*, 90, 332-338,
738 10.2134/agronj1998.00021962009000030004x, 1998.
- 739 Böhlenius, H., Huang, T., Charbonnel-Campaa, L., Brunner, A. M., Jansson, S., Strauss, S. H., and Nilsson,
740 O.: CO/FT regulatory module controls timing of flowering and seasonal growth cessation in trees,
741 *Science*, 312, 1040-1043, 10.1126/science.1126038, 2006.
- 742 Bolte, A., Czajkowski, T., Coccozza, C., Tognetti, R., de Miguel, M., Psidova, E., Ditmarova, L., Dinca, L.,
743 Delzon, S., Cochard, H., Raebild, A., de Luis, M., Cvjetkovic, B., Heiri, C., and Muller, J.: Desiccation and
744 Mortality Dynamics in Seedlings of Different European Beech (*Fagus sylvatica* L.) Populations under
745 Extreme Drought Conditions, *Front Plant Sci*, 7, 751, 10.3389/fpls.2016.00751, 2016.
- 746 Brelsford, C. C., Trasser, M., Paris, T., Hartikainen, S. M., and Robson, T. M.: Understorey light quality
747 affects leaf pigments and leaf phenology in different plant functional types, *bioRxiv*, 829036,
748 10.1101/829036, 2019.
- 749 Brunner, I., Herzog, C., Dawes, M. A., Arend, M., and Sperisen, C.: How tree roots respond to drought,
750 *Front Plant Sci*, 6, 547, 10.3389/fpls.2015.00547, 2015.

751 Buck, A. L.: New Equations for Computing Vapor Pressure and Enhancement Factor, *Journal of Applied*
752 *Meteorology*, 20, 1527-1532, 10.1175/1520-0450(1981)020<1527:Nefcvp>2.0.Co;2, 1981.

753 Bultot, F., Coppens, A., and Dupriez, G. L.: Estimation de l'évapotranspiration potentielle en Belgique :
754 (procédure révisée), Bruxelles : Institut royal météorologique de Belgique, 1983.

755 Campioli, M., Verbeeck, H., Van den Bossche, J., Wu, J., Ibrom, A., D'Andrea, E., Matteucci, G., Samson,
756 R., Steppe, K., and Granier, A.: Can decision rules simulate carbon allocation for years with contrasting
757 and extreme weather conditions? A case study for three temperate beech forests, *Ecol. Model.*, 263, 42-
758 55, 10.1016/j.ecolmodel.2013.04.012, 2013.

759 Carrara, A., Kowalski, A. S., Neirynek, J., Janssens, I. A., Yuste, J. C., and Ceulemans, R.: Net ecosystem
760 CO₂ exchange of mixed forest in Belgium over 5 years, *Agricultural and Forest Meteorology*, 119, 209-
761 227, [https://doi.org/10.1016/S0168-1923\(03\)00120-5](https://doi.org/10.1016/S0168-1923(03)00120-5), 2003.

762 Chelle, M., Evers, J. B., Combes, D., Varlet-Grancher, C., Vos, J., and Andrieu, B.: Simulation of the three-
763 dimensional distribution of the red:far-red ratio within crop canopies, *New Phytol.*, 176, 223-234,
764 <https://doi.org/10.1111/j.1469-8137.2007.02161.x>, 2007.

765 Chiang, C., Olsen, J. E., Basler, D., Bankestad, D., and Hoch, G.: Latitude and Weather Influences on Sun
766 Light Quality and the Relationship to Tree Growth, *Forests*, 10, 610, ARTN 610
767 10.3390/f10080610, 2019.

768 Crabbe, R. A., Dash, J., Rodriguez-Galiano, V. F., Janous, D., Pavelka, M., and Marek, M. V.: Extreme
769 warm temperatures alter forest phenology and productivity in Europe, *Sci Total Environ*, 563-564, 486-
770 495, 10.1016/j.scitotenv.2016.04.124, 2016.

771 De Boeck, H. J., and Verbeeck, H.: Drought-associated changes in climate and their relevance for
772 ecosystem experiments and models, *Biogeosciences*, 8, 1121-1130, 10.5194/bg-8-1121-2011, 2011.

773 De Boeck, H. J., De Groot, T., and Nijs, I.: Leaf temperatures in glasshouses and open-top chambers,
774 *New Phytol*, 194, 1155-1164, 10.1111/j.1469-8137.2012.04117.x, 2012.

775 De Vos, B.: Capability of PlantCare Mini-Logger technology for monitoring of soil water content and
776 temperature in forest soils: test results of 2015, *Reports of Research Institute for Nature and Forest*,
777 *Instituut voor Natuur- en Bosonderzoek*, 85 pp., 2016.

778 Estiarte, M., and Penuelas, J.: Alteration of the phenology of leaf senescence and fall in winter deciduous
779 species by climate change: effects on nutrient proficiency, *Glob. Chang. Biol.*, 21, 1005-1017,
780 10.1111/gcb.12804, 2015.

781 Fox, J., and Weisberg, S.: *An {R} Companion to Applied Regression*, Third ed., Sage, Thousand Oaks (CA),
782 2019.

783 Fracheboud, Y., Luquez, V., Bjorken, L., Sjodin, A., Tuominen, H., and Jansson, S.: The control of autumn
784 senescence in European aspen, *Plant Physiol.*, 149, 1982-1991, 10.1104/pp.108.133249, 2009.

785 Franklin, K. A., and Quail, P. H.: Phytochrome functions in Arabidopsis development, *J. Exp. Bot.*, 61 1,
786 11-24, 2010.

787 Fu, Y., Campioli, M., Vitasse, Y., De Boeck, H., Berge, J., Abdelgawad, H., Asard, H., Piao, S., Deckmyn, G.,
788 and Janssens, I.: Variation in leaf flushing date influences autumnal senescence and next year's flushing
789 date in two temperate tree species, *Proc Natl Acad Sci U S A*, 111, 10.1073/pnas.1321727111, 2014.

790 Fu, Y. H., Piao, S., Delpierre, N., Hao, F., Hänninen, H., Liu, Y., Sun, W., Janssens, I. A., and Campioli, M.:
791 Larger temperature response of autumn leaf senescence than spring leaf-out phenology, *Global Change*
792 *Biol.*, 24, 2159-2168, <https://doi.org/10.1111/gcb.14021>, 2018.

793 Gallinat, A. S., Primack, R. B., and Wagner, D. L.: Autumn, the neglected season in climate change
794 research, *Trends Ecol Evol*, 30, 169-176, 10.1016/j.tree.2015.01.004, 2015.

795 Gárate-Escamilla, H., Brelford, C. C., Hampe, A., Robson, T. M., and Garzón, M. B.: Greater capacity to
796 exploit warming temperatures in northern populations of European beech is partly driven by delayed

797 leaf senescence, *Agricultural and Forest Meteorology*, 284, 107908, 10.1016/j.agrformet.2020.107908,
798 2020.

799 Garnier, S.: viridis: Default Color Maps from 'matplotlib'. 2018.

800 Gill, A. L., Gallinat, A. S., Sanders-DeMott, R., Rigden, A. J., Short Gianotti, D. J., Mantooth, J. A., and
801 Templer, P. H.: Changes in autumn senescence in northern hemisphere deciduous trees: a meta-analysis
802 of autumn phenology studies, *Ann. Bot.*, 116, 875-888, 10.1093/aob/mcv055, 2015.

803 Hastie, T., and Tibshirani, R.: Generalized Additive Models, *Statistical Science*, 1, 297-310, 1986.

804 Holm, G.: Chlorophyll Mutations in Barley, *Acta Agric Scand*, 4, 457-471, 10.1080/00015125409439955,
805 1954.

806 Hörtensteiner, S., and Feller, U.: Nitrogen metabolism and remobilization during senescence, *J. Exp.*
807 *Bot.*, 53, 927-937, 10.1093/jexbot/53.370.927, 2002.

808 Hothorn, T., Bretz, F., and Westfall, P.: Simultaneous Inference in General Parametric Models, *Biom J*,
809 50, 346-363, 2008.

810 IPCC: Climate change 2014: synthesis report. Contribution of Working Groups I, II and III to the fifth
811 assessment report of the Intergovernmental Panel on Climate Change. Core Writing Team, R. K. P. a. L.
812 A. M. e. (Ed.), IPCC, Geneva, Switzerland, 2014.

813 Kassambara, A.: ggpubr: 'ggplot2' Based Publication Ready Plots. 2019.

814 Keskitalo, J., Bergquist, G., Gardstrom, P., and Jansson, S.: A cellular timetable of autumn senescence,
815 *Plant Physiol.*, 139, 1635-1648, 10.1104/pp.105.066845, 2005.

816 Kint, V., Aertsens, W., Campioli, M., Vansteenkiste, D., Delcloo, A., and Muys, B.: Radial growth change of
817 temperate tree species in response to altered regional climate and air quality in the period 1901–2008,
818 *Clim. Change*, 115, 343-363, 10.1007/s10584-012-0465-x, 2012.

819 KMI: Klimatologisch seizoenoverzicht, lente 2017, 2017a.

820 KMI: Klimatologisch seizoenoverzicht, herfst 2017, 2017b.

821 KMI: Klimatologisch seizoenoverzicht, zomer 2017, 2017c.

822 KMI: Klimatologisch seizoenoverzicht, herfst 2018, 2018a.

823 KMI: Klimatologisch seizoenoverzicht, zomer 2018, 2018b.

824 KMI: Klimatologisch seizoenoverzicht, herfst 2019, 2019a.

825 KMI: Klimatologisch seizoenoverzicht, zomer 2019, 2019b.

826 Kobayashi, Y., and Weigel, D.: Move on up, it's time for change - Mobile signals controlling photoperiod-
827 dependent flowering, *Genes Dev.*, 21, 2371-2384, 10.1101/gad.1589007, 2007.

828 Koike, T.: Autumn coloring, photosynthetic performance and leaf development of deciduous broad-
829 leaved trees in relation to forest succession, *Tree Physiology*, 7, 21-32, 10.1093/treephys/7.1-2-3-4.21,
830 1990.

831 Koornneef, M., Hanhart, C. J., and van der Veen, J. H.: A genetic and physiological analysis of late
832 flowering mutants in *Arabidopsis thaliana*, *Mol Gen Genet*, 229, 57-66, 10.1007/bf00264213, 1991.

833 Kwon, J., Khoshimkhujiev, B., Lee, J., Ho, I., Park, K., and Choi, H. G.: Growth and Yield of Tomato and
834 Cucumber Plants in Polycarbonate or Glass Greenhouses, *Korean Journal of Horticultural*
835 *Science&Technology*, 35, 79-87, 10.12972/kjhst.20170009, 2017.

836 Legris, M., Klose, C., Burgie, E. S., Rojas, C. C. R., Neme, M., Hiltbrunner, A., Wigge, P. A., Schäfer, E.,
837 Vierstra, R. D., and Casal, J. J.: Phytochrome B integrates light and temperature signals in
838 Arabidopsis, *Science*, 354, 897, 10.1126/science.aaf5656, 2016.

839 Legris, M., Ince, Y., and Fankhauser, C.: Molecular mechanisms underlying phytochrome-controlled
840 morphogenesis in plants, *Nat Commun*, 10, 5219, 10.1038/s41467-019-13045-0, 2019.

841 Leul, M., and Zhou, W.: Alleviation of waterlogging damage in winter rape by application of uniconazole:
842 Effects on morphological characteristics, hormones and photosynthesis, *Field Crops Res.*, 59, 121-127,
843 [https://doi.org/10.1016/S0378-4290\(98\)00112-9](https://doi.org/10.1016/S0378-4290(98)00112-9), 1998.

844 Leuzinger, S., Zotz, G., Asshoff, R., and Korner, C.: Responses of deciduous forest trees to severe drought
845 in Central Europe, *Tree Physiol*, 25, 641-650, 10.1093/treephys/25.6.641, 2005.

846 Mancinelli, A. L., and Rabino, I.: The "High Irradiance Responses" of Plant Photomorphogenesis, *Bot.*
847 *Rev.*, 44, 129-180, 1978.

848 Mariën, B., Balzarolo, M., Dox, I., Leys, S., Lorene, M. J., Geron, C., Portillo-Estrada, M., AbdElgawad, H.,
849 Asard, H., and Campioli, M.: Detecting the onset of autumn leaf senescence in deciduous forest trees of
850 the temperate zone, *New Phytol*, 224, 166-176, 10.1111/nph.15991, 2019.

851 Matile, P.: Biochemistry of Indian summer: physiology of autumnal leaf coloration, *Exp Gerontol*, 35,
852 145-158, [https://doi.org/10.1016/S0531-5565\(00\)00081-4](https://doi.org/10.1016/S0531-5565(00)00081-4), 2000.

853 Medawar, P. B.: *The Uniqueness of the individual*, by P.B. Medawar, Methuen, London, 1957.

854 Menzel, A., Helm, R., and Zang, C.: Patterns of late spring frost leaf damage and recovery in a European
855 beech (*Fagus sylvatica* L.) stand in south-eastern Germany based on repeated digital photographs, *Front*
856 *Plant Sci*, 6, 110, 10.3389/fpls.2015.00110, 2015.

857 Michelson, I. H., Ingvarsson, P. K., Robinson, K. M., Edlund, E., Eriksson, M. E., Nilsson, O., and Jansson,
858 S.: Autumn senescence in aspen is not triggered by day length, *Physiol Plant*, 162, 123-134,
859 10.1111/ppl.12593, 2018.

860 Munné-Bosch, S., and Alegre, L.: Die and let live: leaf senescence contributes to plant survival under
861 drought stress, *Funct. Plant Biol.*, 31, 10.1071/fp03236, 2004.

862 Neff, M. M., Fankhauser, C., and Chory, J.: Light: an indicator of time and place, *Genes Dev*, 14, 257-271,
863 2000.

864 Niinemets, Ü.: Responses of forest trees to single and multiple environmental stresses from seedlings to
865 mature plants: Past stress history, stress interactions, tolerance and acclimation, *For. Ecol. Manage.*,
866 260, 1623-1639, 10.1016/j.foreco.2010.07.054, 2010.

867 Novick, K. A., Ficklin, D. L., Stoy, P. C., Williams, C. A., Bohrer, G., Oishi, A. C., Papuga, S. A., Blanken, P.
868 D., Noormets, A., Sulman, B. N., Scott, R. L., Wang, L. X., and Phillips, R. P.: The increasing importance of
869 atmospheric demand for ecosystem water and carbon fluxes, *Nature Climate Change*, 6, 1023-1027,
870 10.1038/Nclimate3114, 2016.

871 Pedersen, E. J., Miller, D. L., Simpson, G. L., and Ross, N.: Hierarchical generalized additive models in
872 ecology: an introduction with mgcv, *PeerJ*, 7, e6876, 10.7717/peerj.6876, 2019.

873 Penman, H. L.: Natural evaporation from open water, bare soil and grass, *Proc R Soc Lond A Math Phys*
874 *Sci*, 193, 120-145, 10.1098/rspa.1948.0037, 1948.

875 Poorter, H., Niinemets, Ü., Ntagkas, N., Siebenkäs, A., Mäenpää, M., Matsubara, S., and Pons, T.: A meta-
876 analysis of plant responses to light intensity for 70 traits ranging from molecules to whole plant
877 performance, *New Phytol.*, 223, 1073-1105, <https://doi.org/10.1111/nph.15754>, 2019.

878 Pšidová, E., Ditmarová, L., Jamnická, G., Kurjak, D., Majerová, J., Czajkowski, T., and Bolte, A.:
879 Photosynthetic response of beech seedlings of different origin to water deficit, *Photosynthetica*, 53,
880 187-194, 10.1007/s11099-015-0101-x, 2015.

881 R Core Team: *R: A language and environment for statistical computing*. R Foundation for Statistical
882 Computing, Vienna, Austria, 2020.

883 Richardson, A. D., Keenan, T. F., Migliavacca, M., Ryu, Y., Sonnentag, O., and Toomey, M.: Climate
884 change, phenology, and phenological control of vegetation feedbacks to the climate system, *Agricultural*
885 *and Forest Meteorology*, 169, 156-173, 10.1016/j.agrformet.2012.09.012, 2013.

886 Rigby, R. A., and Stasinopoulos, D. M.: Generalized additive models for location, scale and shape, *Journal*
887 *of the Royal Statistical Society Series C-Applied Statistics*, 54, 507-544, DOI 10.1111/j.1467-
888 9876.2005.00510.x, 2005.

889 Rose, N. L., Yang, H., Turner, S. D., and Simpson, G. L.: An assessment of the mechanisms for the transfer
890 of lead and mercury from atmospherically contaminated organic soils to lake sediments with particular
891 reference to Scotland, UK, *Geochim. Cosmochim. Acta*, 82, 113-135, 10.1016/j.gca.2010.12.026, 2012.

892 Schulze, E.-D., Beck, E., Buchmann, N., Clemens, S., Müller-Hohenstein, K., and Scherer-Lorenzen, M.:
893 Plant Ecology, 2019.

894 Seyednasrollah, B., Young, A. M., Li, X., Milliman, T., Ault, T., Frohling, S., Friedl, M., and Richardson, A.
895 D.: Sensitivity of Deciduous Forest Phenology to Environmental Drivers: Implications for Climate Change
896 Impacts Across North America, *Geophys. Res. Lett.*, 47, e2019GL086788, 10.1029/2019gl086788, 2020.

897 Simpson, G. L.: gratia: Graceful 'ggplot'-Based Graphics and Other Functions for GAMs Fitted Using
898 'mgcv'. 2020.

899 Smith, H.: Light Quality, Photoperception, and Plant Strategy, *Annual Review of Plant Physiology*, 33,
900 481-518, 10.1146/annurev.pp.33.060182.002405, 1982.

901 Turcsan, A., Steppe, K., Sarkozi, E., Erdelyi, E., Missoorten, M., Mees, G., and Mijnsbrugge, K. V.: Early
902 Summer Drought Stress During the First Growing Year Stimulates Extra Shoot Growth in Oak Seedlings
903 (*Quercus petraea*), *Front Plant Sci*, 7, 193, 10.3389/fpls.2016.00193, 2016.

904 Van den Berge, J., Naudts, K., Zavalloni, C., Janssens, I. A., Ceulemans, R., and Nijs, I.: Altered response to
905 nitrogen supply of mixed grassland communities in a future climate: a controlled environment
906 microcosm study, *Plant Soil*, 345, 375-385, 10.1007/s11104-011-0789-8, 2011.

907 van der Werf, G. W., Sass-Klaassen, U. G. W., and Mohren, G. M. J.: The impact of the 2003 summer
908 drought on the intra-annual growth pattern of beech (*Fagus sylvatica* L.) and oak (*Quercus robur* L.) on a
909 dry site in the Netherlands, *Dendrochronologia*, 25, 103-112, 10.1016/j.dendro.2007.03.004, 2007.

910 Vander Mijnsbrugge, K., Turcsan, A., Maes, J., Duchene, N., Meeus, S., Steppe, K., and Steenackers, M.:
911 Repeated Summer Drought and Re-watering during the First Growing Year of Oak (*Quercus petraea*)
912 Delay Autumn Senescence and Bud Burst in the Following Spring, *Front Plant Sci*, 7, 419,
913 10.3389/fpls.2016.00419, 2016.

914 Vitasse, Y., François, C., Delpierre, N., Dufrêne, E., Kremer, A., Chuine, I., and Delzon, S.: Assessing the
915 effects of climate change on the phenology of European temperate trees, *Agricultural and Forest
916 Meteorology*, 151, 969-980, 10.1016/j.agrformet.2011.03.003, 2011.

917 Vito, M., and Muggeo, R.: segmented: an R Package to Fit Regression Models with Broken-Line
918 Relationships, *R News*, 8, 20-25, 2008.

919 Vonwettstein, D.: Chlorophyll-letale und der submikroskopische Formwechsel der Plastiden, *Exp. Cell
920 Res.*, 12, 427-506, 10.1016/0014-4827(57)90165-9, 1957.

921 Wang, S., Yang, B., Yang, Q., Lu, L., Wang, X., and Peng, Y.: Temporal Trends and Spatial Variability of
922 Vegetation Phenology over the Northern Hemisphere during 1982-2012, *PLoS ONE*, 11, e0157134,
923 10.1371/journal.pone.0157134, 2016.

924 Wickham, H.: ggplot2: Elegant Graphics for Data Analysis, Springer-Verlag, New York, 2009.

925 Wickham, H., François, R., Henry, L., and Müller, K.: dplyr: A Grammar of Data Manipulation. 2018.

926 Wilke, C. O.: cowplot: Streamlined Plot Theme and Plot Annotations for 'ggplot2'. 2019.

927 Willems, P.: Compound intensity/duration/frequency-relationships of extreme precipitation for two
928 seasons and two storm types, *Journal of Hydrology*, 233, 189-205, 10.1016/s0022-1694(00)00233-x,
929 2000.

930 Willems, P.: Multidecadal oscillatory behaviour of rainfall extremes in Europe, *Clim. Change*, 120, 931-
931 944, 10.1007/s10584-013-0837-x, 2013.

932 Wolfe, B. T., Sperry, J. S., and Kursar, T. A.: Does leaf shedding protect stems from cavitation during
933 seasonal droughts? A test of the hydraulic fuse hypothesis, *New Phytol*, 212, 1007-1018,
934 10.1111/nph.14087, 2016.

935 Wood, S. N.: Fast stable restricted maximum likelihood and marginal likelihood estimation of
936 semiparametric generalized linear models, *J. Roy. Stat. Soc. Ser. B. (Stat. Method.)*, 73, 3-36,
937 10.1111/j.1467-9868.2010.00749.x, 2011.

938 Xie, Y., and Wilson, A. M.: Change point estimation of deciduous forest land surface phenology, *Remote
939 Sens. Environ.*, 240, 111698, 10.1016/j.rse.2020.111698, 2020.

940 Yanovsky, M. J., and Kay, S. A.: Molecular basis of seasonal time measurement in Arabidopsis, *Nature*,
941 419, 308-312, 10.1038/nature00996, 2002.
942 Zeileis, A., and Hothorn, T.: Diagnostic Checking in Regression Relationships, *R News*, 2, 7-10, 2002.
943 Zeng, H., Jia, G., and Epstein, H.: Recent changes in phenology over the northern high latitudes detected
944 from multi-satellite data, *Environmental Research Letters*, 6, 045508, 10.1088/1748-9326/6/4/045508,
945 2011.
946 Zuur, A., Ieno, E., and Smith, G.: *Analysing Ecological Data*, *Statistics for Biology and Health*, 2007.
947 Zuur, A. F., Ieno, E. N., and Elphick, C. S.: A protocol for data exploration to avoid common statistical
948 problems, *Methods Ecol. Evol.*, 1, 3-14, 10.1111/j.2041-210X.2009.00001.x, 2010.
949 Zuur, A. F., Ieno, E. N., and Freckleton, R.: A protocol for conducting and presenting results of regression-
950 type analyses, *Methods Ecol. Evol.*, 7, 636-645, 10.1111/2041-210x.12577, 2016.

951